



Universidad Autónoma de Querétaro

Faculty of Engineering

Master of Science in
Artificial Intelligence

Three-dimensional Digitization and Reconstruction of the Human Face Using Fringe Analysis by Phase-Shifting.

THESIS

A thesis submitted for the degree of
Master of Science in Artificial Intelligence

By:

Luis Arturo Alvarado Escoto

Supervisor:

Dr. Jesús Carlos Pedraza Ortega

SYNODS

Dr. Jesús Carlos Pedraza Ortega

President

Dr. Marco Antonio Aceves Fernández

Secretary

Dr. Juan Manuel Ramos Arreguin

Vocal

Dr. Saúl Tovar Arriaga

Alternate

Dr. Efrén Gorrostieta Hurtado

Alternate

Centro Universitario
Querétaro, QRO
Mexico.
January 2021

Dirección General de Bibliotecas UAQ

This thesis is dedicated to my family

Acknowledgment

To Conacyt for the scholarship given for two years, which allowed me to complete the master of science in artificial intelligence at the Autonomous University of Queretaro.

To my family, for all the support given to me during every moment of this two year journey. Without their love, patience and support, I wouldn't have been able to accomplish this.

To my friends who were with me in every step of the way, thank you for making my time easier during these two years.

To my professors, for passing on their knowledge onto us and sharing their time and experiences with me. Especially, thank you to my thesis director: Dr. Jesus Carlos Pedraza Ortega, I couldn't have chosen a better person to lead me during this time. Thank you for mentoring, listening, helping and putting up with me. You are an example of discipline, responsibility, equity and teamwork.

Abstract

This thesis proposes a methodology to successfully reconstruct surfaces, especially the human face, in 3D parting from two dimensional images. By using fringe analysis and phase-shifting profilometry, a 3D representation of surfaces can be achieved, modeling its real dimensions and characteristics.

The proposed methodology adds to the traditional phase-shifting algorithms by introducing two stages. The first is the detection of region of interest by image segmentation using K-means and binary morphology, which reduces the propagation of noise during the phase unwrapping stage. The second, introduces a cross filter during the post-processing stage that improves the visual quality of the reconstructed surface by reducing or attenuating the presence of Moiré patterns.

Throughout this document a highly detailed explanation of the proposed methodology is presented. Also, the algorithms for two main contributions are shown, as well as an analysis of some of the more common phase unwrapping algorithms. These algorithms were evaluated in terms of speed and accuracy.

The results showed that the proposed methodology obtains better reconstructions in terms of image quality and real height measurement than the traditional method. Furthermore, the introduction of noise filtering as a post-processing stage reduces the presence of Moiré patterns, whose presence is due to the utilization of the phase-shifting technique, resulting in better height estimations and visually high quality 3D reconstructions.

Keywords: Computer Vision, 3D Reconstruction, Profilometry, Phase Shifting, Moiré patterns, Phase Unwrapping, K-means, 3D measurement, Cross-Filter.

Contents

Acknowledgment

Abstract

1	Introduction	1
1.1	Computer Vision	1
1.2	Backgroud and related work	2
1.3	State of the art	4
1.4	Problem statement	6
1.5	Justification	6
1.6	Hypothesis	7
1.7	Objectives	7
1.7.1	General objective	7
1.7.2	Specific objectives	7
1.8	Scope and limitations	8
1.8.1	Scope	8
1.8.2	Limitations	8
1.9	Thesis organization	8
2	Literature review	10
2.1	Three-dimensional reconstruction	10
2.2	Fringe projection analysis	12
2.3	Phase-shifting interferometry	14
2.4	Phase extraction	15
2.5	Phase unwrapping	16
2.6	Moiré patterns	17

3	Methodology	20
3.1	Phase-shifting profilometry	22
3.1.1	Three-step algorithm	22
3.2	Image acquisition	22
3.3	Image pre-processing	25
3.3.1	Histogram equalization	25
3.3.2	Gamma correction	26
3.4	Detection of Region of interest	27
3.4.1	Image segmentation by K-means	28
3.4.2	Binary Morphology	31
3.5	Phase Extraction	33
3.6	Phase unwrapping	33
3.6.1	Phase unwrapping algorithms	35
3.6.2	Analysis of phase unwrapping algorithms	36
3.7	Filtering	39
3.7.1	Cross filter	39
4	Results	42
4.1	Database	42
4.2	3D reconstructions	44
4.3	Impact of ROI detection and cross filtering	47
4.3.1	Shadow detection	48
4.3.2	Cross filtering up close	49
4.4	Comparative with other methods	51
5	Conclusions and future work	54
5.1	Conclusions	54
5.2	Recommendations for Future Work	55
	References	57

Dirección General de Bibliotecas UAG

List of Figures

2.1	Taxonomy of 3D profilometry techniques (Escobar, 2016).	11
2.2	Taxonomy of optical techniques used for three-dimensional information extraction of surfaces (Escobar, 2016).	11
2.3	A typical profilometry by fringe projection setup (Gorthi & Rastogi, 2010)	12
2.4	Examples of fringe projection patterns.	13
2.5	Steps to achieve 3D reconstruction using PSP	15
2.6	Wrapped phase effect on a 1D signal (Gdesait & Lilley, 2012)	16
2.7	Image displaying Moiré patterns	18
2.8	Comparative of an original profile and after adding Moiré noise	19
3.1	Proposed methodology	21
3.2	Sinusoidal waves used to create the fringe patterns	23
3.3	Capture setup	24
3.4	Example of images captured in the image acquisition stage for the three-step method	25
3.5	Example of histogram equalization where the histogram is equally distributed	26
3.6	Example of gamma correction for different values of γ	27
3.7	Detection of ROI using K-means and binary morphology	27
3.8	Image segmentation using K-means	29
3.9	Segmentation using K-means with different values of K	29
3.10	Obtainment of the binary mask from the segmented image.	31
3.11	Example of captured after detection of ROI	33
3.12	2D representation of the wrapped phase maps	34
3.13	3D representation of the wrapped phase maps	34
3.14	Example of synthetic objects used for phase unwrapping analysis	37
3.15	Example of symmetric objects used for testing	38

3.16	Analysis by profile of the performance of PU algorithms in symmetric objects	38
3.17	Cross filtering	40
3.18	Steps to apply cross filter to an image	40
4.1	Example of some of the surfaces used for testing	43
4.2	3D reconstruction of an object by stages, visualization in 2D.	44
4.3	3D reconstruction of an object	45
4.4	3D reconstruction of a human face, visualization in 2D.	46
4.5	3D reconstruction of an object	47
4.6	Impact of ROI detection and cross filtering in a highly detailed surface	48
4.7	Example of shadow exclusion by image segmentation	49
4.8	A closer look at Moiré noise treatment by cross filter	50
4.9	Profile analysis of a 3D reconstruction before and after applying cross filter	51
4.10	Comparative of a reconstructed surface by various methods visualized in 2D. . . .	52
4.11	Comparative of a reconstructed surface by various methods visualized in 3D. . . .	52

Dirección General de Bibliotecas UAQ

List of Tables

1.1	State of the art of 3D reconstruction related works	5
3.1	Metrics for the phase unwrapping algorithms using symmetric objects	37
3.2	Metrics for the phase unwrapping algorithms using symmetric objects	37
4.1	Devices used for image acquisition	42
4.2	Height metrics comparative with other methods	53

Dirección General de Bibliotecas UAQ

Introduction

The world is visualized in three dimensions. Conventional cameras and image detectors can only capture the intensity information from a scene in two dimensions, but are unable to obtain the shape and depth of an object or scene. Just as humans can appreciate the world tridimensionally through the eyes, intelligent vision systems must have the means to obtain the 3D information of a scene through input images. To face this challenge, 3D measurement technologies have developed a number of techniques that allow to obtain the quantitatively geometric data in three dimensions parting from bi-dimensional input images.

This thesis presents an approach to 3D measurement and 3D reconstruction by using phase-shifting profilometry in complex surfaces, as it is the human face. Different techniques were implemented and evaluated, specially in the phase unwrapping and post-processing steps. The used methodology to achieve a successful reconstruction of the face is described in detail. The images used for the experiments were captured using a typical profilometry by fringe projection setup. This work also proposes a filter to reduce the presence of Moiré patterns in the achieved reconstructions as a post-processing stage in the 3D reconstruction process.

1.1 Computer Vision

Humans perceive the three-dimensional structure of the world in an effortlessly way. Computer vision seeks to help computers “see” and understand content in imagery the way that living beings do. In computer vision, researchers try to describe the world in one or more images and to reconstruct its properties, such as shape, illumination, color among others. Computer vision, as a field of artificial intelligence, intends to recreate the human capabilities in a computer of accurately identifying

and locating objects and the react to what is “seen” using digital images and video (Szeliski, 2010).

Although the difficulty of computer vision has been underestimated by many, recent developments and its use in a wide variety of real-world applications, have turned it into one of the great pillars of artificial intelligence. Such applications include but are not limited to:

- Optical character recognition
- Machine inspection
- Retail
- 3D model building
- Medical imaging
- Automotive Safety
- Biometrics
- 3D modeling
- Face detection
- Visual authentication

Optical profilometry is one of the main areas of research in computer vision and the main topic of this work (Szeliski, 2010).

1.2 Background and related work

Surface profilometry has been constantly evolving over the last few decades, quickly becoming a boom subject for research. Thus, existing tridimensional reconstruction and 3D measurement techniques have been modified and improved and new and modern ones have been proposed offering improvements over the traditional methods. Thanks to these techniques, 3D reconstructions are now more detail-clear, precise and with greater resolution(Gorthi & Rastogi, 2010).

Structured light-based techniques have proven more popular among researchers for the extraction of the real world measurement information of a surface. This, given their low computational

cost and high resolution. A typical light-based profilometry system consists of a LCD (liquid crystal display) unit projecting a pattern of fringes over a surface, and a camera in charge of capturing the image of the object and the projected fringes (Sansoni, Corini, Lazzari, Rodella, & Docchio, 1997). An alternate system proposed by Pan Ou allows to simultaneously capture bi-dimensional color texture and tridimensional measurement in real time. This set-up proposes to replace the LCD projector by a DLP (digital light processing) unit and set a second camera to obtain captures of the object in full color(Ou, Li, Wang, & Zhang, 2013).

One of the more crucial factors when using a structured light-based profilometry system is the creation of the fringe patterns that are to be projected over the object. Although there are a number of methods such as, color coded projections, sequential projections and gray-scale indexation (Van der Jeught & Dirckx, 2016), *Fourier Transform* techniques have proven most effective since they require as little as one capture in order to obtain the 3D profile of the surface. Using a sinusoid pattern makes the system to be less sensitive to image defocus when compared to the other methods. Takeda(Takeda & Mutoh, 1983) proposed that the fringes be sinusoid and that they be projected over the object to appear deformed by the shape of the surface of the object when captured from a certain angle with the camera. Alternate methods based of Fourier Transform are phase-shifting and wavelet transform techniques (Zaid, 2008). Wavelet transform techniques splits the signal in segments, allowing detection of the local characteristics of the fringe pattern resulting in more precise measurements. However, this technique has proven to be more costly computationally. Zaid proposes a method by working with a Morlet Wavelet to extract the phase of the fringe patters using phase and frequency estimation. Numerous tests using wavelet transform over the human face as a complex surface (Mohammadi, Madanipour, & Rezaie, 2012) have been performed, improving on the measurements of noise induced patterns. The complement method consists of two steps, noise reduction and phase extraction.

Although the aforementioned methods allow to generate 3D measurements of surfaces to low costs, speed plays a major factor in the desire to propose new methodologies that would create more precise reconstructions and greater speeds. Gong's method reports to have obtained measurements of a surface to a speed rate of 400 Hz with an exposition of 8 μ s. The method utilizes a DLP¹ projector and Fourier Transform for the creation and projection of the fringe patterns. Allegedly, the proposed method eliminates bottlenecks in traditional methods by using binary structured fringe pattern(Gong & Zhang, 2010).

¹Digital Light Processing

For the tridimensional digitization of the face Nguyen proposes a method that does not require active lighting or artificial patterns. The technique is based on binocular stereo image and digital image correlation (Nguyen, Kieu, Wang, & Le, 2018). One of the main steps of the technique is image comparison, for this, and to achieve a reliable comparison of pixel to pixel, the pores and freckles of the skin are used for the characteristics of patterns, which facilitates the process. The main advantage of this method is the practicality with which the images are obtained since only two calibrated cameras are needed to obtain reliable digitization, with results similar to active techniques such as fringe analysis, unlike other techniques where the system configuration takes longer.

Surface profilometry techniques are still in constant evolution given the technological advances being developed and the demand by the industry and the scientific field to generate reconstructions that are detailed and that match the real measurements of the object. However, complex surfaces, as is the human face, are still challenging for even the more sophisticated methods.

1.3 State of the art

Phase-shifting profilometry is in constant development and over recent years many authors have introduced different approaches to this area of research. Table 1.1 shows some recent works related to 3D reconstruction using PSP, as well as new approaches to the phase unwrapping stage, especially those based on AI² techniques.

²Artificial Intelligence

Table 1.1: State of the art of 3D reconstruction related works

Author	Technique	Use of the technique	Contribution
Escobar R. (2016)	Phase-shifting profilometry	3D reconstruction of computer generated objects	Eliminate discontinuities in phase different to 2π
Moya Morales JC (2017)	Amplitude spectrum analysis	State of the art of filters used in the analysis of the amplitude spectrum	Comparison of different filters used in the two-dimensional Fourier amplitude spectrum for 3D reconstruction using Fourier transform
Sun Y. (2018)	Convolutional neural networks	Noise reduction	Moiré pattern reduction and smoothing using deep convolutional networks.
An Y. & Zhong S. (2018)	Phase extraction	Phase unwrapping	Proposed method to obtain the unwrapped phase using a low-cost 3D scanner to capture 3D information from the scene and transform it into a real coordinate system.
Law B. & Lun D.P.K. (2019)	Deep Learning	Deep learning for phase extraction	Use of deep learning for phase extraction using a single fringe image. The phase is extracted using a single deep network.
Guangkai F. (2019).	3D extraction	Profilometry based on tri-color binary stripes.	3D reconstruction system using a single RGB stripe pattern.
Lopez-Torres C & Pedraza-Ortega JC (2020)	Shadow region detection	3D reconstruction by wavelet transform	Improves the accuracy of 3D reconstruction by detecting and removing shadow regions in 3D wavelet transform measurements
Sen X. (2020).	SVM	Phase unwrapping using SVM ³	Use of SVM for phase splitting in 3D profilometry. The phase splitting problem is solved as a classification problem.

³ Support vector machine

1.4 Problem statement

The use of 3D modeling of the human face in facial authentication systems, video games, security systems and graphical interfaces have turned facial tridimensional reconstruction into one of the more active areas of research in optical profilometry and computer vision (Salvi, Fernandez, Pribanic, & Llado, 2010). However, unlike objects whose features are static and do not depend on external factors that change their characteristics, facial reconstruction can be particularly tricky and still present complications in terms of resolution and detail capturing due to the number of specific features that differ from face to face. Features such as shape, head size, facial expressions and age generated traits, facial hair among others create shadows and holes in the generated reconstructions (Yagnik, Siva, Ramakrishnan, & Rao, 2005). Each face must be treated as a unique surface, therefore making the task of reconstruction harder.

The measurement of the surface of the human face is a current challenge faced by 3D reconstructions techniques. Given the unicity of each individual's face and the feature variation that an image can obtain of the same facial surface from another, it is extremely difficult to standardize a method for extraction of 3D information of this particular surface. External factors, such as gestures, the angle from which the capture was taken, the amount of light reflected onto the surface, facial imperfections and obstructions to name a few, make that the reconstructed surface and the acquired information obtained by the reconstructions and the applied techniques, to vary from other captures of the exact same face, generating inexact, and non-reliable reconstructions.

Systems based on facial reconstruction in the industry, such as video games and facial recognition security systems, although improved, still present inaccurate and untrustworthy reconstructions, capable of giving security and trust to users. Given that the face can have a number of interpretations due to the external factors to which is exposed, 3D facial reconstructions systems present a great area of opportunity and improvement by giving the created model much more certainty and accuracy.

1.5 Justification

There are currently a large number of research areas in computer vision and optical metrology, dedicated to the development and improvement of profilometry techniques that lead to the reconstruction in three dimensions of the face. 3D facial reconstruction is mainly applied on facial

authentication and recognition systems, in the video game industry, for the creation of personalized avatars, in the development of virtual reality, in movies, medicine and a multitude of disciplines within the engineering ambit. There has been a great increase in the development of facial reconstruction-based systems, given the ease of use, customization and reliability that these systems may offer to their users, specifically, the security that can be placed on them as in the case of facial authentication systems.

Many known methods used in optical profilometry are applied to the reconstruction of objects and of the face, it is important to study, test and improve over these techniques in order to successfully recreate more accurate, precise and trustworthy reconstructions, taking always into account the factors affecting the face of a person. Improve on the current techniques for 3D facial reconstruction and propose new ones will lead to generate better results and therefore 3D reconstructions that can be used on a professional environment (Gorthi & Rastogi, 2010).

1.6 Hypothesis

Using phase-shifting profilometry and phase unwrapping techniques, a tridimensional representation of objects and of the human face can be achieved parting from a set of bi-dimensional images, accurately modeling the real features and dimensions of the facial surface.

1.7 Objectives

1.7.1 General objective

Improve on the 3D reconstruction and modeling systems of objects and of the human face through an algorithm based on phase-shifting profilometry applying fringe pattern analysis and introducing artificial intelligence algorithms and post-processing filters.

1.7.2 Specific objectives

- Review existing fringe projection and phase unwrapping methods.
- Create tridimensional images of object, especially human faces, applying phase shifting profilometry techniques.

- Implement an algorithm based on phase-shifting profilometry and gray scale fringes to obtain the real measurements of the face and the needed information to generate a tridimensional surface.
- Implement and test different phase unwrapping algorithms, especially those based on artificial intelligence techniques.
- Improve on the results by testing different filters to remove Moiré noise.

1.8 Scope and limitations

1.8.1 Scope

- Follow up on the topic of 3D reconstruction by phase-shifting profilometry as an effective technique of acquiring the 3D information of objects and the human face.
- Develop an algorithm based on phase-shifting profilometry and including AI techniques for ROI⁴ detection and phase unwrapping.
- Create a database for testing and for future related works.
- Propose a methodology for 3D extraction based on PSP⁵ that includes a pre-processing and post-processing stages.
- Do the appropriate test and experiments in every step of the project to conclude the work.

1.8.2 Limitations

- Lack of a dedicated laboratory with low light for imaging tests.
- Built structure for image acquisition.

1.9 Thesis organization

The first chapter briefly describes the project, its objectives, justification, related work, hypothesis and the scope and limitations.

⁴Region of interest

⁵Phase-shifting profilometry

The second chapter of this document presents the literature review necessary for the understanding of certain terms such as: fringe analysis, phase extraction, phase unwrapping, phase-shifting, Moiré patterns etc.

The third and most extensive chapter describes in detail the proposed methodology to achieve a 3D reconstruction of surfaces using PSP. It describes the steps for the acquisition of the images, the detection of ROI, the phase treatment and the post-processing stages. It also describes the metrics used to measure the precision of the results. Finally, it presents an analysis of some of the more commonly used phase unwrapping algorithms and presents their effectiveness and speed.

The obtained results and presented in chapter 4. Here, certain test cases of computer generated and real object as well as human faces are analyzed. Also, a comparison with other methodologies can be found here.

Finally, chapter 5 concludes on the contributions of the research as well as the future work that could still be done to further improve on the methodology.

Literature review

2.1 Three-dimensional reconstruction

Three-dimensional reconstruction can be defined as the process by which a 3D representation of an object, or the surface of an object can be obtained, parting from one or multiple 2D views, maintaining the real-world characteristics of the object, such as depth, volume and shape(Vila, Arranz, & Alvar, 2009).

Three-dimensional information extraction techniques can be divided into two groups; by contact and by non-contact. Contact techniques requires a friction with the working surface; therefore, their greatest disadvantage lies in the lack of precision to extract information from soft or deformable objects. On the other side, non-contact techniques do not require any friction with the surface. A taxonomy of 3D profilometry techniques can be found in figure 2.1.

Among non-contact techniques, optical measurement is the more common. These techniques have a subdivision of their own, passive and active; figure 2.2 shows a classification of optical techniques and their subdivisions. In passive approaches, the scene is imaged by two or more cameras and correspondences between the images are found to extract the 3D shape. On the other side, active techniques replaces one of the cameras by and active device, a projector, which projects a light pattern onto the scene. The projected pattern imposes the illusion of texture onto the object, increasing the number of correspondences, thus obtaining dense reconstruction for textureless surfaces (Fernandez & Salvi, 2013).

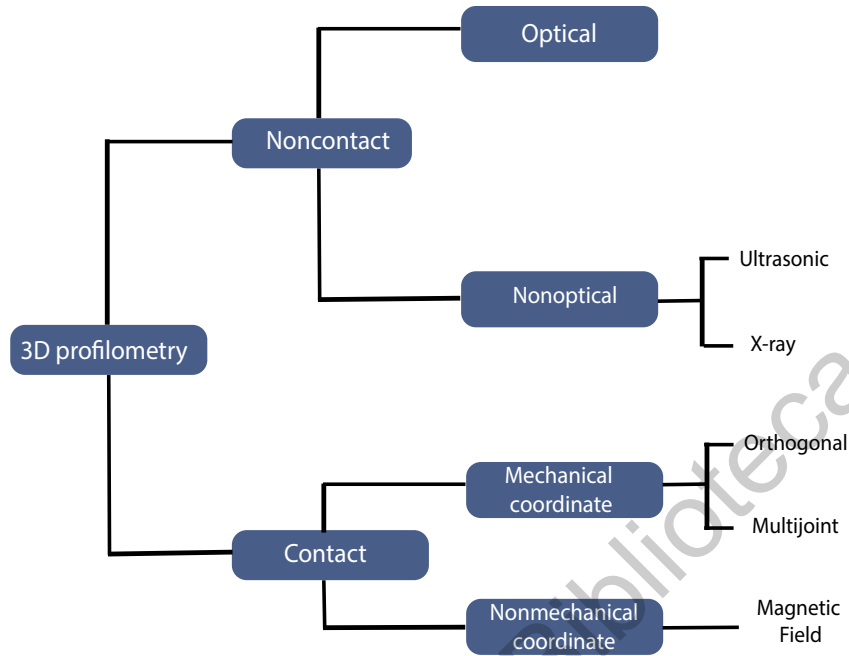


Figure 2.1: Taxonomy of 3D profilometry techniques (Escobar, 2016).

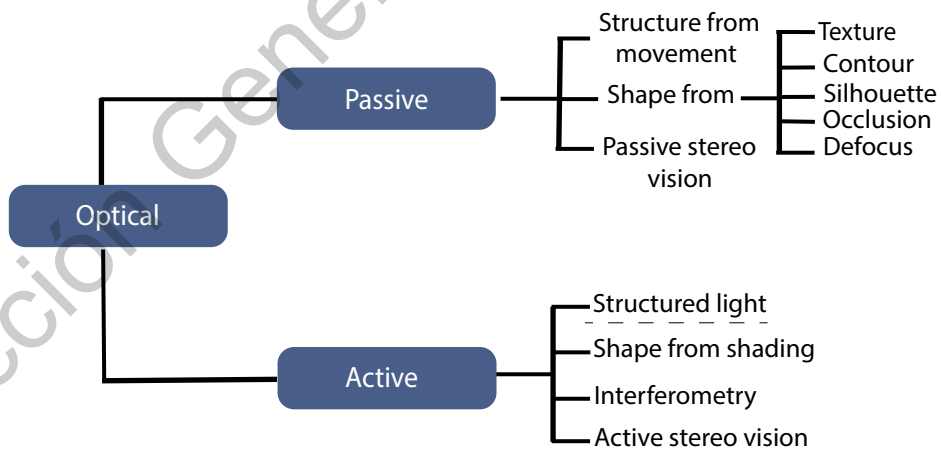


Figure 2.2: Taxonomy of optical techniques used for three-dimensional information extraction of surfaces (Escobar, 2016).

Active optical techniques, specially structured light techniques, are more commonly used since they have proven to be more effective and less costly. Extraction by structured light, also called active triangulation, is based on two premises, codified projected light and sinusoidal fringe patterns techniques. Through this method, object depth is extracted by projecting a deformed fringe pattern over the object. (Jun-ichi, 2015).

2.2 Fringe projection analysis

The main idea behind fringe projection is to obtain the height map from a certain object as a deformed fringe pattern at the same time as obtaining a contour map. The acquired fringe pattern allows to visualize the physical characteristics of the object, although it is necessary to extract the qualitative conditions of these patterns for metrological purposes.(Jun-ichi, 2015).

A typical profilometry by fringe projection system is shown in figure 2.3. A generated fringe pattern is projected onto the object or the surface on which the 3D extraction is being performed. Using a camera, images of the demodulated fringe patterns are captured, later, an analysis of these images is done in order to digitize and reconstruct the object. Just as shown in figure 2.3 triangulation between the projector's angle, the camera and the object under analysis allows to obtain the object's depth.

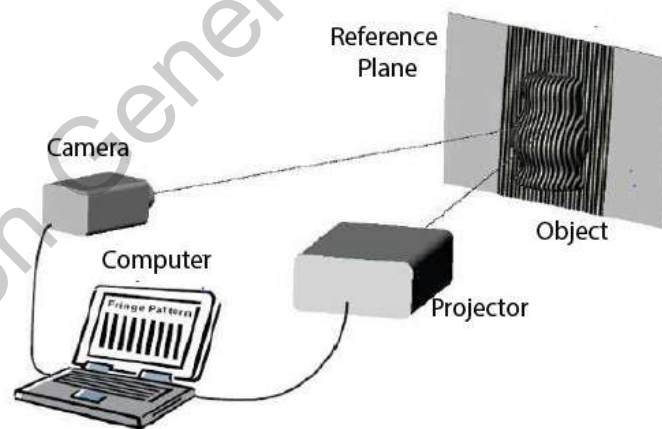


Figure 2.3: A typical profilometry by fringe projection setup (Gorthi & Rastogi, 2010)

Many different patterns are used in fringe projection, squares, diamonds, hexagons, among others, but fringes are the most common. Although in general, these fringes are found vertically,

they can be also used horizontally or diagonally. An example of this patterns can be seen in figure 2.4.

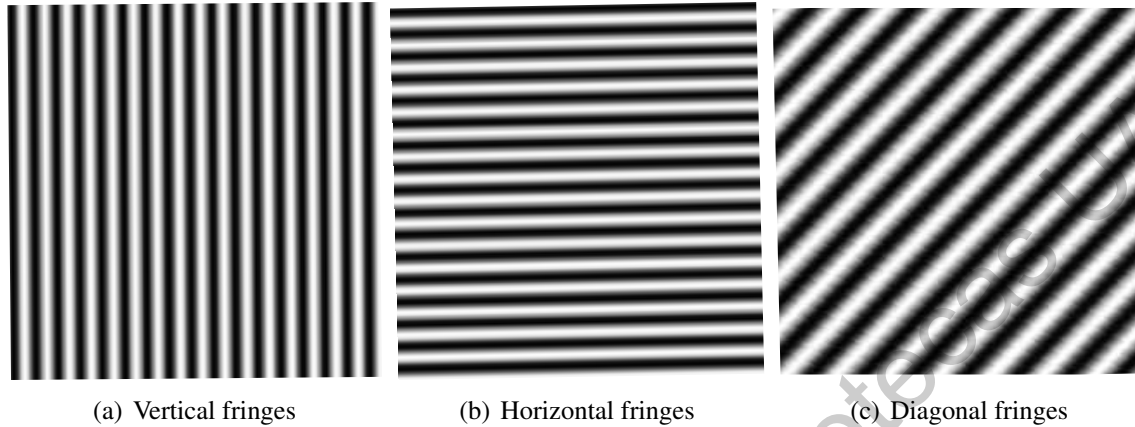


Figure 2.4: Examples of fringe projection patterns.

Typically, a sine wave pattern is projected, where every vertical line represents a unique phase value in the frequency domain (Dai, Li, & Zhang, 2014). Conventionally, sine patterns are used due to the mathematical treatment that can be given to them. In theory, an image of sine fringes $I(x,y)$ can be expressed as equation 2.1.

$$I(x,y) = a(x,y) + b(x,y)\cos(\phi(x,y)) \quad (2.1)$$

Where $I(x,y)$ is the average intensity, $b(x,y)$ represents the modulation depth of the fringes in a field of vision and $\phi(x,y)$ is the phase distribution.

There are many sophisticated methods based on fringe projection analysis to extract the tridimensional information of a solid, such as phase-shifting and Fourier transforms. These methods can be classified depending on the number of input image patterns used for phase extraction (Junichi, 2015).

1. One input image, in which only one fringe pattern image is captured and analyzed.
2. Multiple input images, in which at least three patterns are used whose initial phase is shifted by a given value.

Among the more common one image techniques are: Wavelet transform profilometry (WTP), spatial filtered profilometry (SFP) and Fourier transform profilometry (FTP). FTP is the most com-

monly used technique when only one input image is used. In FTP, a Ronchi ruling of sinusoidal pattern is projected onto the surface. The depth information, which is encoded into the deformed fringe pattern, can be decoded by calculating Fourier transformation, filtering in spatial frequency domain and by calculating the inverse Fourier transformation. One of its main advantages is that it requires no fringe interpolation, since it gives height distribution at every pixel over the entire field(Xianyu & Chen, 2001).

2.3 Phase-shifting interferometry

The phase-shifting method is the most popular fringe analysis method using multiple input images. Phase-shifting techniques are used for phase extraction and are widely applied in optical metrology due to their velocity and efficiency. When using phase-shifting, multiple fringe patterns with their initial phase shifted by a given value are acquired by some means. The phase-shifted fringe pattern images are captured at different times or sampling spaces.

In principle, having a greater number of samples decreases the noise in the intensity, which leads into greater accuracy in the obtained measurements. In phase-shifting profilometry, a series of fringe patterns are captured while the reference phase in the fringe pattern shifts. The absolute phase is then encoded in the variations in the intensity pattern, and the phase can be retrieved by a simple point to point calculation. The intensity in each point may vary as a sine function of the induced shift in the phase (Schreiber & Bruning, 2006).

The merit of PSP is that the phase value to be measured can be extracted by a pixel-by-pixel operation. Thus, the accuracy of phase calculation can be improved by increasing the number of samples. On the other hand, since it is necessary to acquire multiple images at different timings, it is easily influenced by surrounding disturbances such as vibrations and movements. This means, that the phase-shifting method may not be suitable for an instantaneous measurement of objects in motion(Jun-ichi, 2015). The steps to follow to obtain a 3D representation of an object using PSP are shown in figure 2.5

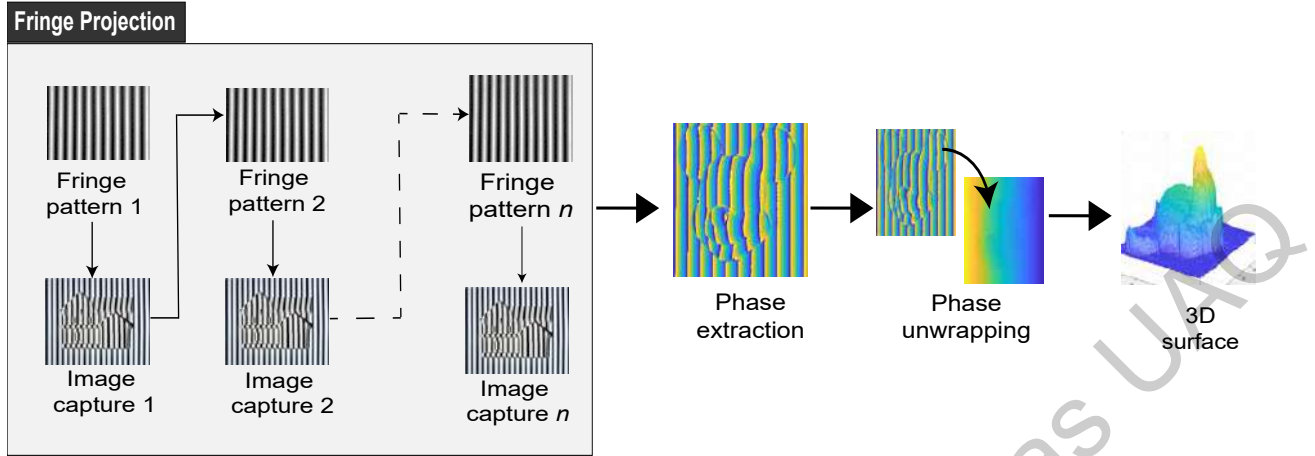


Figure 2.5: Steps to achieve 3D reconstruction using PSP

Some of the more traditional phase-shifting methods are the *three-step* and *four-step*, named by the number of input images required. Another commonly used method is the *double three-step* which takes the traditional *three-step* method and applies it twice with an initial phase offset of 60 degrees between them, and the two obtained phase maps are averaged to generate the final phase map (Huang, Hu, & Chiang, 2002).

Generally, a *N-step* method can be described. For the sampling number $k = 1, 2, \dots, N$, the N images of fringe intensity pattern can be expressed in the form given by equation 2.2.

$$I(x, y) = a(x, y) + b(x, y) \cos(\phi(x, y) + (k - 1)\delta) \quad (2.2)$$

Where, ϕ is the phase to solve. The phase is normally fixed and given by $\delta = \frac{2\pi}{N}$ where N is the number of input images.

2.4 Phase extraction

To obtain the height of the surface, the information immersed in the phase must be extracted. When taking the *N-step* method and by using all the images, the relation between the phase map $\phi(x, y)$ and the intensity values at each pixel is deduced by the equation 2.3 (Jun-ichi, 2015).

$$\phi(x, y) = \tan^{-1} \frac{\sum_{k=1}^N I_k(x, y) \sin[(k-1)\delta]}{\sum_{k=1}^N I_k(x, y) \cos[(k-1)\delta]} \quad (2.3)$$

The phase map obtained will be known as *wrapped phase* map. This, given the nature of the arctan function which mathematically limits the extracted values to the interval $[-\pi, +\pi]$. The real phase may very well range over an interval greater than 2π , meaning that the recovered phase contains artificial discontinuities. In order to restore the extracted phase to its true values, an additional step known as phase unwrapping must take place.

2.5 Phase unwrapping

The *wrapped phase* map contains discontinuous phase jumps between adjacent pixels from $+\pi$ to $-\pi$ or its opposite direction. Therefore, a procedure to connect the discontinuous phase jumps becomes necessary for obtaining the final physical distribution. Mathematically, the wrapped phase can be expressed as equation 2.4. Figure 2.6 shows the effect of wrapping on a 1D continuous phase signal.

$$x_w(n) = W[x(n)] \quad (2.4)$$

Where $x(n)$ is the original continuous phase, $W[]$ in the wrapped phase operator and $x_w(n)$ is the wrapped phase.

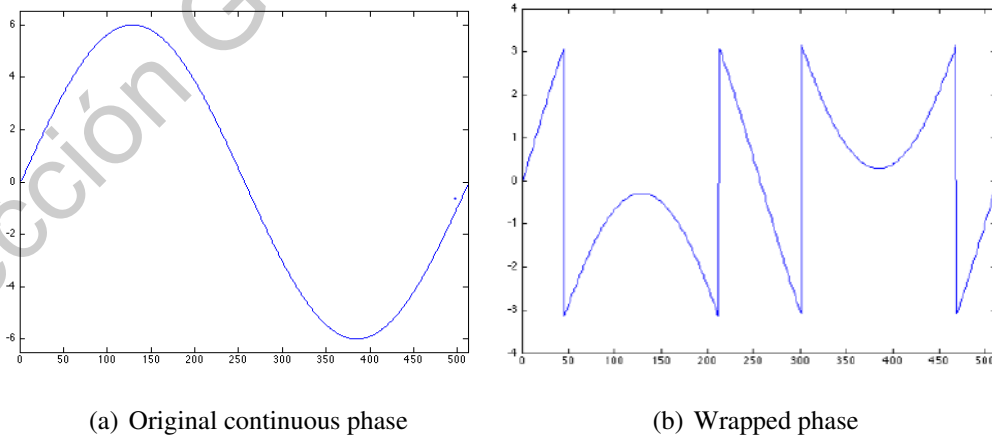


Figure 2.6: Wrapped phase effect on a 1D signal (Gdesait & Lilley, 2012)

Phase unwrapping is a process that refers to determining the unknown integral multiple of 2π that will be added to each pixel of the wrapped phase, previously acquired, to make it continuous in the frequency domain. Thus, removing all the artificial 2π discontinuities obtained as a result of applying the arctangent function to obtain the phase. This process is carried out by comparing the phase of neighboring pixels and adding or subtracting 2π to bring the relative phase between both pixels to a range of $-\pi$ to $+\pi$. Phase unwrapping is a complete NP problem and it's turned difficult due to the presence of shadows, low fringe modulations, fringe discontinuities, noise in the images, among others (Gorthi & Rastogi, 2010)

Over the years, a number of phase unwrapping methods and techniques have been developed used to correct the phase discontinuities. In fringe analysis, phase unwrapping algorithms can be divided into two main categories (Jun-ichi, 2015):

1. **Algorithms based on minimum spanning tree:** Methods to obtain a continuous trace of phase unwrapping, spanning the effective phase area with trajectories in tree-shaped paths with no localized closed loop. To select the most effective path, cost functions, such as the spatial phase and fringe contrast are used, in order to decide the reliability of the pixels.
2. **Algorithms based on energy minimization:** Methods to obtain the optimum state of phase unwrapping by minimizing an energy function, based on the sum of the differences of the phases of neighboring pixels, where the initial phase distribution corresponds to the maximum state of energy. The energy function is converged to the minimum energy state by varying the phases at all pixels by $\pm 2\pi$ using some rule. This methods require many iterations and do not depend on the unwrapping path.

2.6 Moiré patterns

Moiré patterns occur when two or more figures with periodic ruling are made to overlap. For the Moiré patterns to appear, the two patterns must not be completely identical, but must be displaced, shifted or rotated. Moiré patterns usually appear as stripes, ripples, curves or intensity and color superimposed on an image. These patterns can dramatically lower the visual quality of an image (Oster & Nishijima, 1963; Wei, Wang, Nichol, Wiebe, & Chapman, 2011). Figure 2.7 shows an example of an image displaying Moiré patterns.



Figure 2.7: Image displaying Moiré patterns.

Figure 2.8 shows a comparison between a profile taken from figure 2.7 and the original noise-less image. Notice how the noisy profile derives completely from the original profile. This also depends on the severity of the noise, since it is very present in this example, the two profiles show very different characteristics. A lesser intense noisy profile may show a better approximation to its original representation.

Over the years, given the increasing demand for high resolution and detailed clear images, the number of techniques capable of reducing Moiré patterns has been on the rise. Most of these techniques treat the noise in the frequency domain of the image, analyzing the amplitude spectrum and detecting high frequency peaks. Other approaches include convolutional neural networks and sparse matrix decomposition for the treatment of Moiré patterns (Alvarado Escoto, Ortega, Ramos Arreguin, Gorrostieta Hurtado, & Tovar Arriaga, 2020).

In PSP, Moiré patterns appear given the nature of the fringe patterns used. Furthermore, given the complex origination of the noise, it is very difficult to control its appearance during the data acquisition stage. Therefore, a post-processing method must be carried out in order to remove or reduce the noise. Typically, Moiré noise can be altered in the Fourier domain of the image by correcting the amplitude spectrum components altered by the noise. Noise altering can result in smoother surfaces and reduces the error in height estimation since less peaks are present, resulting in better estimations(Wei et al., 2011).

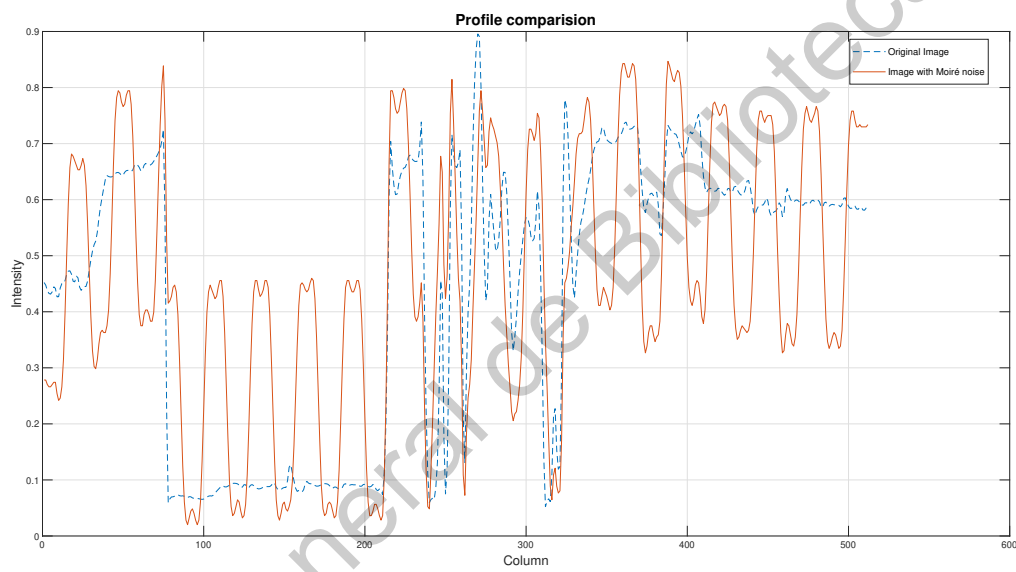


Figure 2.8: Comparative of an original profile and after adding Moiré noise

Methodology

This thesis proposes the use of Phase-shifting profilometry, especially the *three-step* method to successfully obtain a tridimensional representation of surfaces, especially the human face. The implemented methodology describes the steps needed to obtain the 3D information of a surface using PSP. Besides the basic steps needed for 3D reconstruction using PSP as described in the previous chapter, the proposed methodology introduces the detection of the region of interest using clustering algorithms, image pre-processing and the treatment of Moiré patterns in a post-processing stage. This chapter describes in full detail the methods and techniques implemented to achieve a successful 3D reconstruction. Figure 3.1 shows the flow work of every stage of the proposed framework.

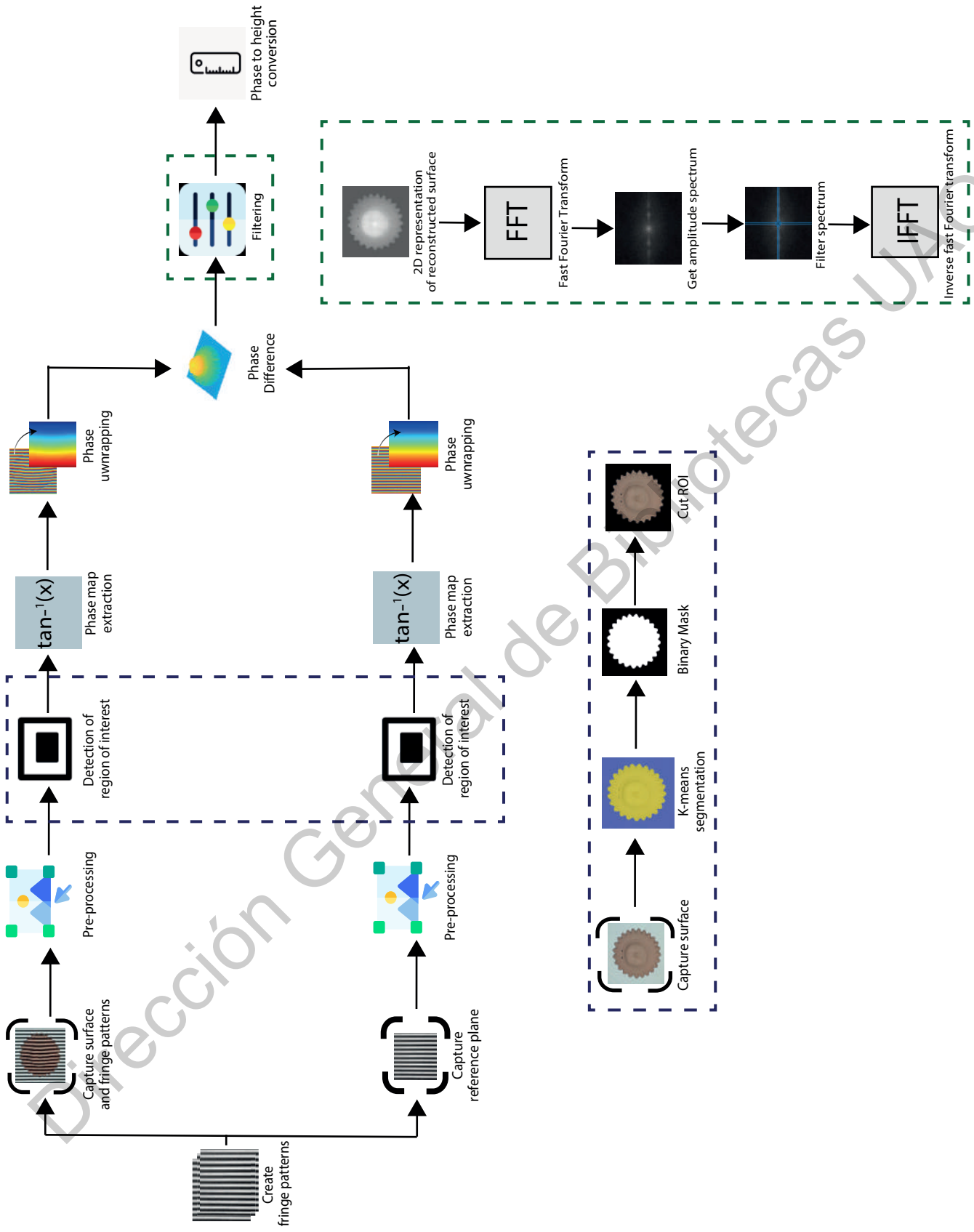


Figure 3.1: Proposed methodology

3.1 Phase-shifting profilometry

3.1.1 Three-step algorithm

One of the most commonly used algorithms in phase-shifting interferometry is the *three-step* method. This technique uses three input images shifted equally. For this method, 90° and 120° are two commonly used phase step sizes. In PSP, the *three-step* algorithm requires the minimum amount of data and is the simplest and fastest to use, but it is also the most sensitive to errors in the phase shift between frames. Equations 3.1, 3.2 and 3.3 describe the patterns used in the three-step algorithm using an offset of 120° (Jun-ichi, 2015).

$$I(x,y) = a(x,y) + b(x,y)\cos(\phi) \quad (3.1)$$

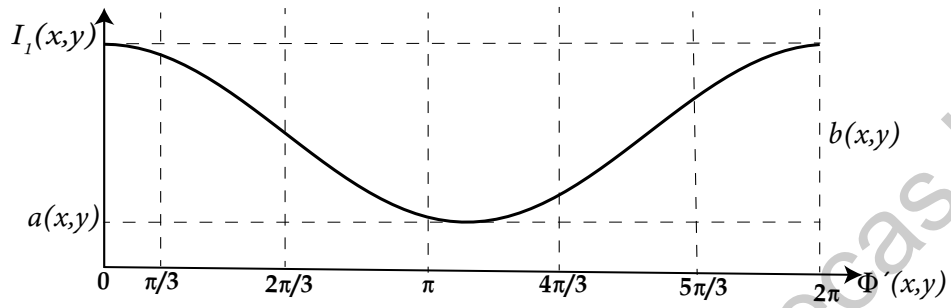
$$I(x,y) = a(x,y) + b(x,y)\cos\left(\phi + \frac{2\pi}{3}\right) \quad (3.2)$$

$$I(x,y) = a(x,y) + b(x,y)\cos\left(\phi + \frac{4\pi}{3}\right) \quad (3.3)$$

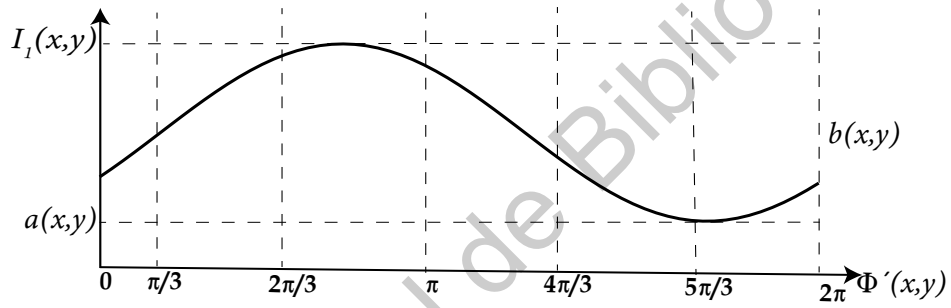
Figure 3.2 shows a graphical representation of the sinusoidal patterns normally used in three-step algorithm. The phase shift between each wave is $\frac{2\pi}{3}$. These shifted waves are mapped over a two-dimensional array to create a fringe pattern image of vertical bars used for fringe projection.

3.2 Image acquisition

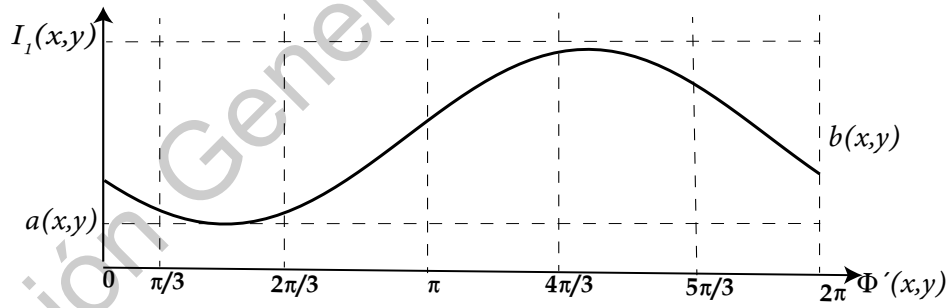
Using a LCD projector, the three fringe patterns are projected onto the surface under study. The object is usually placed facing the projector directly. With the aid of a webcam, which is placed in line with the projector but at a certain distance, each of the deformed fringe patterns are captured. The concept of triangulation is very important, which is why the camera must be placed at an appropriate distance from the projector. Usually the distance between these two devices must be calculated taking into account that the angle between the object and the camera must be around 10° . The setup implemented for this stage can be seen in figure 3.3. On the right of the image the projector can be seen facing the subject, while the camera is positioned to the left of the projector facing the subject with a certain inclination.



(a) ϕ



(b) $\phi + \frac{2\pi}{3}$



(c) $\phi + \frac{4\pi}{3}$

Figure 3.2: Sinusoidal waves used to create the fringe patterns



Figure 3.3: Capture setup

A total of seven images are captured during the image acquisition stage. The first three images are the patterns projected onto the surface. The next three are the reference plane, which are the patterns projected onto the plane where the object or surface is placed. Finally, the seventh image is the object without the fringe patterns projected. This last capture is used for the detection of the ROI⁶. Since ideally, the object is static during the entire acquisition stage, it is expected that the ROI will be located in the same region for every image. The seven images are treated previous to be submitted to the PSP process. The images are cropped and their perspective fixed so that only the region of the object and the fringes is visible. An example of the captured images can be seen in figure 3.4

This stage is essential, since the quality of the images captured will have a great impact in the overall result of the 3D reconstruction. As a recommendation, a white background is used to limit the brightness produced by the projector. It is also important that the objects be as static as possible, since movement may cause differences in the phase-shift which can lead to a bad phase extraction. The experimentation showed that when dealing with faces, the movements or vibrations that the person might make should be limited as possible to avoid error propagation during the process.

⁶Region of Interest

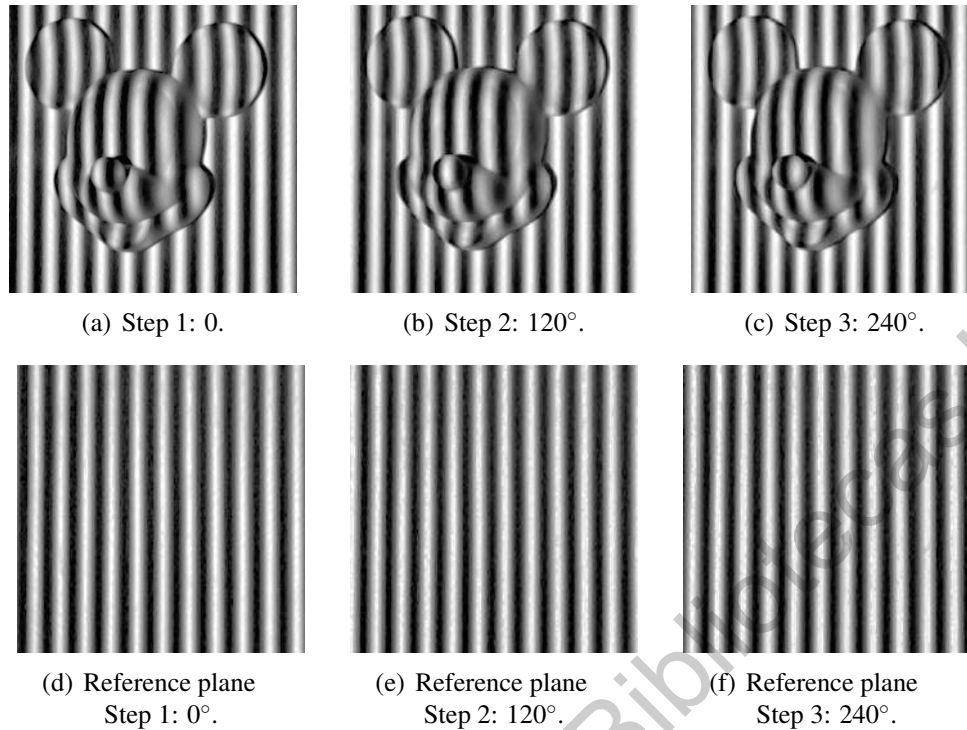


Figure 3.4: Example of images captured in the image acquisition stage for the three-step method

3.3 Image pre-processing

Once the images have been captured they must be treated in order to ease the acquisition of the 3D information. First, the images are converted from RGB to grayscale images, reducing the processing to only one channel. The grayscale images are then normalized to values of $[0.0 - 1.0]$. This would convert the integer values in the images to float values, thus, improving on the precision of calculations. Two operations are used optionally to improve the visual quality of the images: histogram equalization and gamma correction.

3.3.1 Histogram equalization

Histogram equalization is a simple and effective technique for contrast enhancement of images. The histogram equalization flattens and stretches the dynamic ranges of the image's histogram to achieve an overall contrast enhancement. An image with low contrast usually has a narrow histogram located towards the middle of the intensity scale. In a high contrast image, the histogram components cover a much wider range of values in the intensity scale (Raj, Raj, & Kumar, 2015). This, would allow to reduce the brightness created by the LCD projector used during the acquisition.

tion of the images. An example of histogram equalization can be seen in figure 3.5.

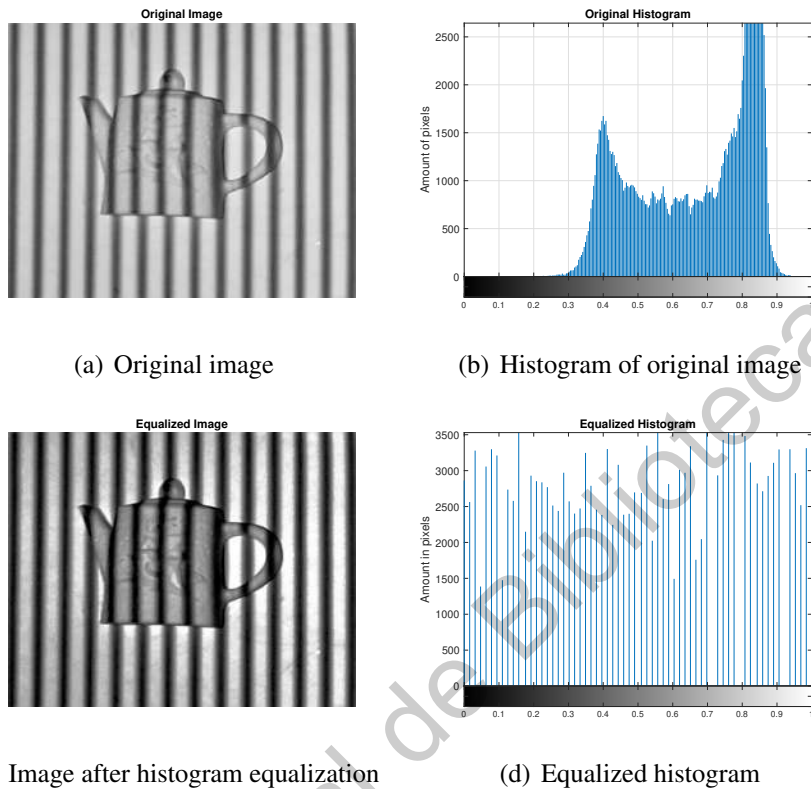


Figure 3.5: Example of histogram equalization where the histogram is equally distributed

In the previous figure, it can be seen that the resulting histogram has a much more uniform distribution covering most of the intensity levels, while the original histogram is inclined towards a certain area of intensity.

3.3.2 Gamma correction

Gamma correction can be used to brighten the fringes from the images captured. Equation 3.4 is used to make the change in the image's gamma values. γ_d represents the desired value, if the value of γ_d is one, the resulting image will be the same as the original, meanwhile, if the value approaches zero, the image will get darker. The gamma non-linearity of the video projector used for image capture decreases the resolution of the images (Guo, He, & Chen, 2004). By correcting the gamma value of the images will improve the luminance conditions of the images. Figure 3.6

shows how the different values of vd affect the original image.

$$\text{gamma} = a^{\frac{1}{vd}} \quad (3.4)$$

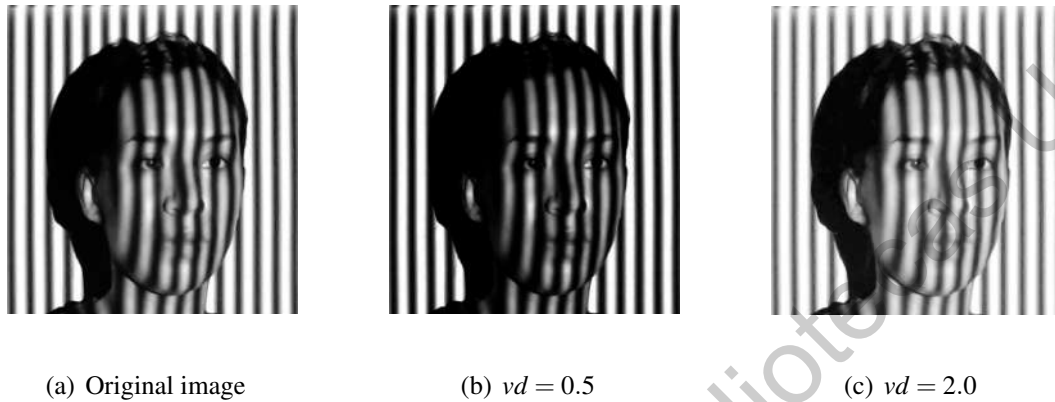


Figure 3.6: Example of gamma correction for different values of vd

3.4 Detection of Region of interest

An important part of the methodology proposed here, is the detection of the region of interest within the images. The main purpose of this is to extract the surface from the images in order to reduce the propagation of error from zones on the images outside the ROI. Once the ROI has been identified, a binary mask is created to map the contour of this region. The binary mask will be used to cut all the images so that only the ROI remains in every one of the captures, see figure 3.7.

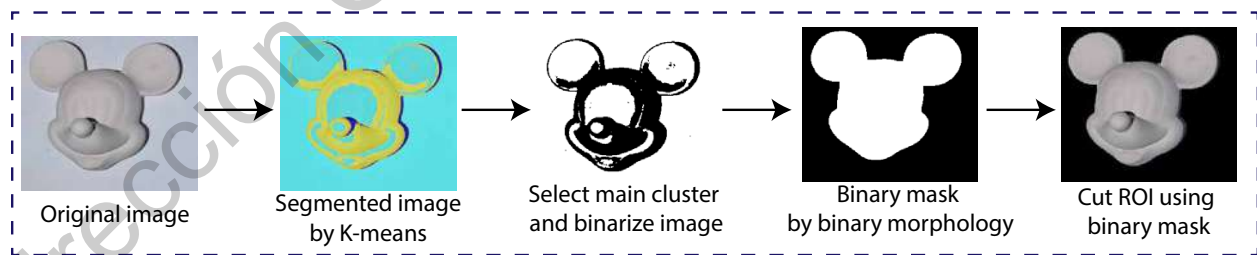


Figure 3.7: Detection of ROI using K-means and binary morphology

3.4.1 Image segmentation by K-means

Image segmentation consists on dividing a digital image on regions named segments. The goal is to simplify the image or change its representation into something that is easier to analyze (Haralick & Shapiro, 1985). Image segmentation allows to detect objects or surfaces in images. By segmenting the image, the region of interest can be easily identified and separated from the rest of the image. Here, a segmentation by K-means algorithm is proposed.

K-means is a clustering algorithm that allows to group a set of data into clusters based on the values of the data and their properties. The goal is to find K groups or clusters among raw data. It is an iterative algorithm that assigns each *point* to one of the K clusters based on its properties. The objective of K-means clustering is to minimize the average squared Euclidean distance between the points and their cluster centers. Equation 3.5 represents the objective function of K-means (Zhao, Deng, & Ngo, 2018) The function $q(\cdot)$ returns the closest centroid for the point x_i .

$$\min \sum_{q(x_i)=r} \|C_r - x_i\|^2 \quad (3.5)$$

It is worth mentioning that the number of clusters is not self-calculated but, must be an input value for the algorithm. In general, there are three steps for clustering (Li & Wu, 2012) :

1. Initialize K cluster centroids
2. Assign each of the points to the closest centroid
3. Recalculate cluster centroids using the points in the cluster

Steps 2 and 3 are repeated iteratively until the convergence is reached or there are no changes in the clusters.

In order to use K-means as a segmentation technique, a RGB image is used to create the dataset used for clustering, see figure 3.8. The RGB image is split into its three channels creating three two-dimensional matrices. The tridimensional points used for clustering are created by taking the values from each of the three channels in the correspondence coordinates. This means that the dataset will contain a total of $m \times n$ points, where m is the height of the image and n its width. Finally, the pixels in the image will be classified based on their color value for segmentation. The value of K is chosen manually depending on the conditions on which the image was captured. When choosing the value of K is important to take into account conditions such as, the color of the

surface, if it is homogeneous or not, the background, and shadow regions. The algorithm for the segmentation of RGB images using K-means is described in algorithm 1.

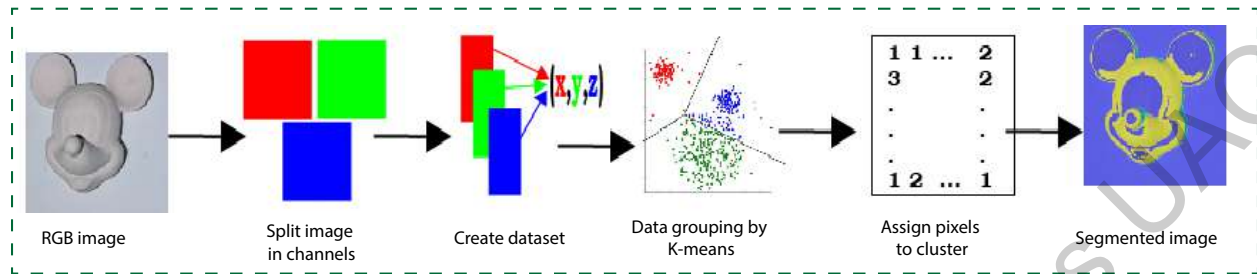


Figure 3.8: Image segmentation using K-means

Algorithm 1 returns a $m \times n$ array containing the labels of the clusters to which each pixel belongs to. It also return the centroids for every cluster. The returning array allows to use color in the original image to detect the regions. An example of image segmentation using k-means can be seen in figure 3.9. In this particular example the value of $K = 2$ offers the better results for image segmentation. Here, we can detect that there are only two regions, since the shape has a uniform color. The segmented images with a value of $K = 3$ and $K = 4$, trims down the surface of the object and leads to a loss of the ROI.

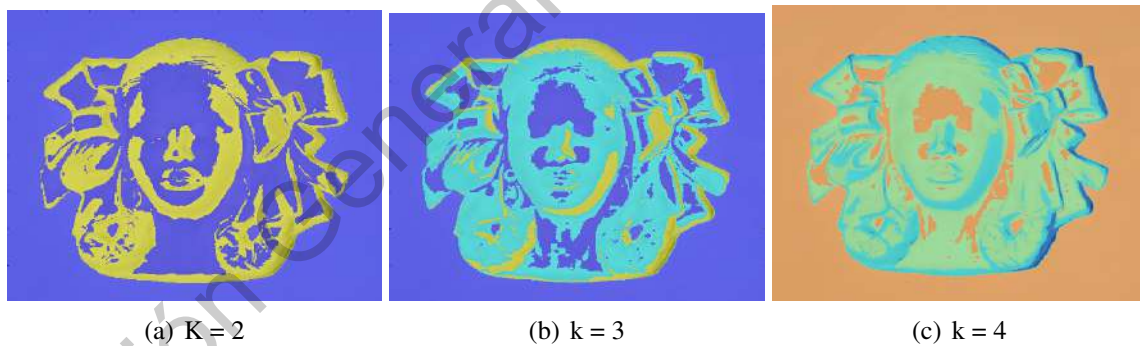


Figure 3.9: Segmentation using K-means with different values of K

Algorithm 1: Image Segmentation by K-means

Input: *Img* - RGB Image

clusters - Number of Clusters

Output: Tags - Two dimensional array of tags

Centroids - Centroids of clusters

```
1 (R,G,B) ← ColorChannelSplit(Img)
2 centroids ← RandomCentroids(3, min, max)
3 prev_tags ← 0
  /* Infinite loop until convergence is reached */
4 while 1 do
5   tags ← 0
6   distances ← 0
7   for i ← 1, ImgWidth do
8     for j ← 2, ImgHeight do
9       for k ← 1, clusters do
10        point ← [R(i,j) G(i,j) B(i,j)]
11        distances(k) ← EuclidianDistance(centroids(k), point)
12        idx ← minimum(distances) // Index of minimum value value
13        tags(i,j) ← idx
14        /* Is convergence reached? */
15      if prev_tags == tags then
16        BREAK
17      else
18        prev_tags ← tags
19      for i ← 1, clusters do
20        Index ← find(tags == i)
21        if idx == empty then
22          centroids(i) ← null
23        else
24          centroid(i) ← findCentroid(R(Index), G(Index), B(Index))
25 return (tags, centroids)
```

3.4.2 Binary Morphology

Parting from the segmented image, the next stage is to construct a binary mask of the ROI which would then be used to cut the rest of the images. The first step to construct this binary mask is to identify the cluster to which most of the ROI belongs to. This is done manually, since K-means arbitrarily assigns labels to the clusters. Once the main cluster is identified, the values belonging to the rest of the clusters are sent to a null value. In figure 3.10 images (a) and (b) show a segmented image and its binary representation once the main cluster has been identified.

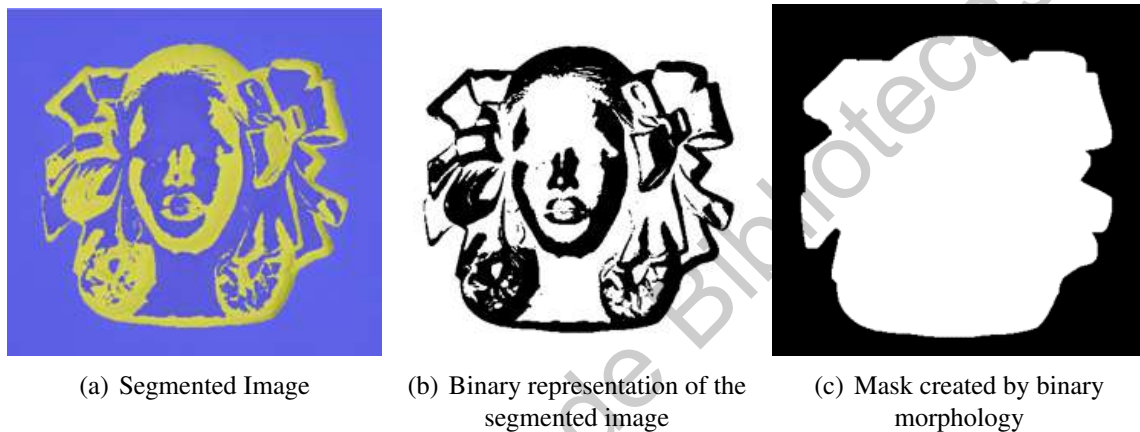


Figure 3.10: Obtainment of the binary mask from the segmented image.

To achieve the binary mask shown in figure 3.10 image (c), binary morphology is used to isolate the silhouette of the object from the rest of the image, closing the region in the best way possible, so that only the ROI remains. Binary morphology is based on set theory. The morphological operations simplify images and keep the most important characteristics of the object's shape. The main idea in binary morphology is to test an image with a simple predefined shape and gather how this shape fits or not in the regions of the image. This simple shape is called a *structuring element* which is a binary image itself (Lin, Si, & Abovslleman, 2007). The morphological operations are described below (Gonzalez, n.d.).

1. **Dilation:** Expands the size of the regions. It is very useful to fill holes or when it is required to join fenced regions that in the image have been separated by poor binarization. When the dilation is performed, the structuring element moves throughout the image and every time the origin of the element coincides with a pixel of value 1 of the original image, all the pixels below it are activated. The dilation will be the union of all these active pixels when the entire

image has been traversed. Dilation is defined as:

$$A \oplus B = \bigcup_{t \in B} A_t = \bigcup_{t \in A} B_t \quad (3.6)$$

2. **Erosion:** Used to separate loosely joined regions or to remove small details. After erosion, only the most significant forms in the regions remain. Viewed more intuitively, when erosion is performed, the structuring element moves throughout the image and each time all the active pixels of the element coincide with a pixel of value 1 of the original image, the pixel below the origin is activated. The erosion will then be the union of all these active pixels when the entire image has been covered. Given a structuring element B , the erosion of an image A can be defined as:

$$A \ominus B = \bigcap_{t \in B} A_{-t} \quad (3.7)$$

3. **Opening:** Erosion followed by dilation with the same structuring element. It is normally used to remove isolated pixels and disconnect loosely joined regions. Opening is defined as:

$$A \circ B = (A \ominus B) \oplus B \quad (3.8)$$

4. **Closing:** A dilation followed by an erosion with the same structuring element. It is normally used when you need to fill spurious holes in some image. Is defined as:

$$A \bullet B = (A \oplus B) \ominus B \quad (3.9)$$

Once the binary mask is created, the six images that were captured with the projected fringe patterns are multiplied pixel by pixel by the binary mask. This will create a new set of images containing only the region of interest and null values around them. An example of this is shown in figure 3.11

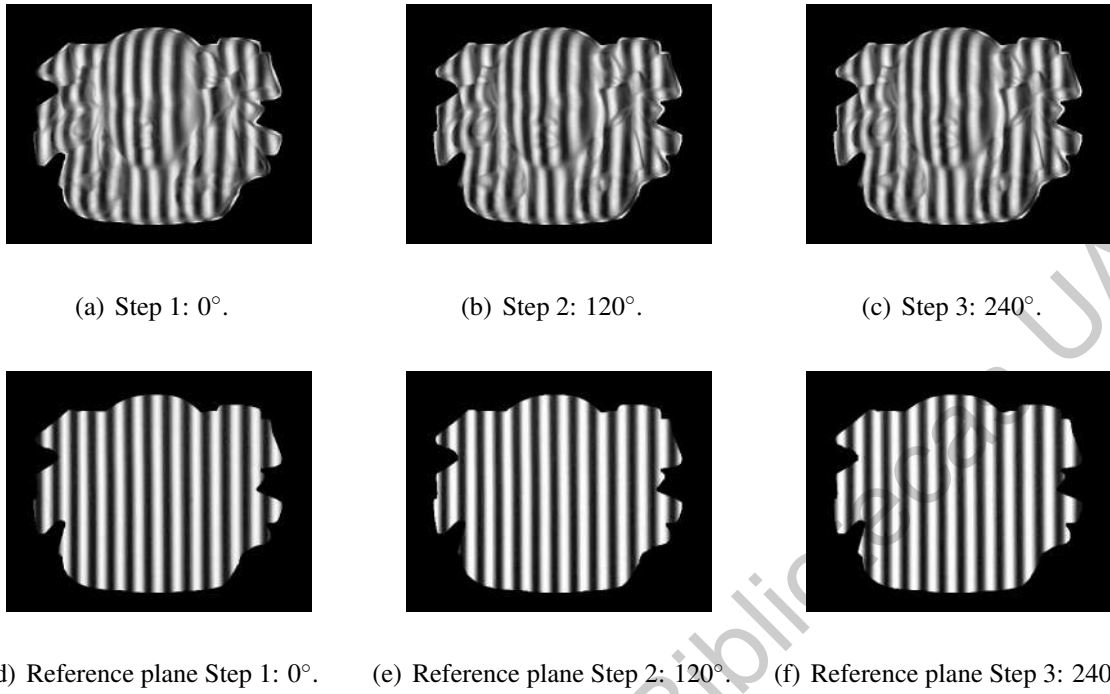


Figure 3.11: Example of captured after detection of ROI

3.5 Phase Extraction

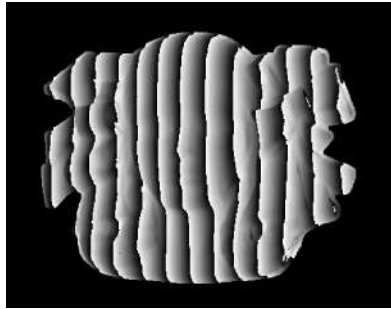
When using *three-step*, equation 2.3 can be simplified, and equation 3.10 can be applied to obtain the absolute phase map.

$$\phi(x,y) = \tan^{-1} \left(\sqrt{3 \frac{I_3(x,y) - I_1(x,y)}{2I_2(x,y) - I_1(x,y) - I_3(x,y)}} \right) \quad (3.10)$$

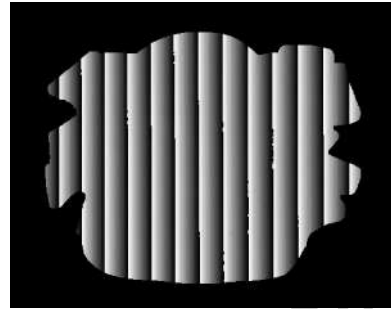
Figures 3.12 and 3.13 show an example of the phase maps extracted using equation 3.10.

3.6 Phase unwrapping

Phase unwrapping is one of the most important steps in 3D reconstruction. Many different methods have been proposed over the years, each based on different techniques and different implementations. For the proposed methodology, some of the most well-known phase unwrapping algorithms were analyzed and tested.

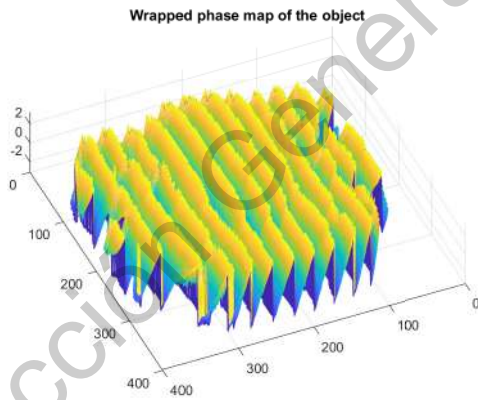


(a) Object

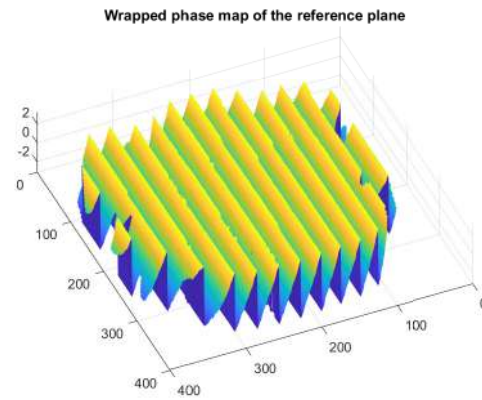


(b) Reference plane

Figure 3.12: 2D representation of the wrapped phase maps



(a) Object



(b) Reference plane

Figure 3.13: 3D representation of the wrapped phase maps

3.6.1 Phase unwrapping algorithms

A brief description of some of the more traditional phase unwrapping algorithms is presented as well as a description of some state of the art techniques.

Itoh 2D phase unwrapping

This algorithm corrects the phase angles in a vector by adding $\pm 2\pi$ when absolute phase jumps are found in consecutive elements. The algorithm unwraps every row of the 2D array, one by one, followed by an unwrapping of the columns of the array. The inverse Itoh algorithm unwraps the columns first, followed then by the rows of the array (Gdesait & Lilley, 2012).

Graph cuts

An energy minimization based algorithm, graph cuts or *PUMA* as it is most commonly known. Here, energy minimization is achieved by a finite sequence of binary minimizations, each one efficiently achieved by a max-flow/min-cut on certain graphs. (Bioucas-Dias & G., 2007).

Constantini phase unwrapping

This technique exploits the fact that discrete derivatives of the wrapped phase are estimated with an error that is an integer multiple of 2π . This leads the phase unwrapping problem to become a minimization problem with integer variables. Here, the deviation between the discrete derivatives and the know derivatives of the wrapped phase, is minimized (Syakrani, Mengko, Suksmono, & E.T., 2007).

Quality Guided

This algorithm is composed of two main steps: create the quality map and the strategy path. The quality map is an imaged based on the phase map, where a weight is give to every pixel according to its changes of successfully unwrapping. On the other hand, the strategy path is order in which every pixel will attempt to unwrap. To represent the quality of a pixel equation is used (Escobar, 2016).

$$\gamma(x, y) = \frac{I''(x, y)}{I'(x, y)} \quad (3.11)$$

3.6.2 Analysis of phase unwrapping algorithms

In order to test the effectiveness of each of the aforementioned PU algorithms. An analysis was performed using two types of objects: synthetic or computer generated and real symmetric objects. Two metrics were used to test their effectiveness in phase unwrapping, *mean squared error* or MSE and *peak signal to noise ratio* or PSNR. Both these metrics were used to compare the final reconstruction using each of the PU algorithms against the original object. Equation 3.12 describes the MSE metric. Here, \hat{y} represent the resulting image, y represents the original input and n is the number of samples, in this case pixels. MSE represents an average difference between the ground truth and the result (Lehmann & Casella, 1998).

$$MSE = \frac{1}{n} \sum (y - \hat{y})^2 \quad (3.12)$$

PSNR usually indicates the maximum energy relation between an original signal and one affected by noise. In images, PSNR can be used to describe the quality of an image when in comparison to another. It is a metric based on MSE and expressed in a logarithmic manner. Thus, a higher PSNR usually means a higher quality in the image. Equation 3.13 describes the way to obtain this metric. Here, the Value of MAX is the maximum possible pixel value of the image (Prof, Saupe, & Hamzaoui, 2001). Since all the results are normalized to a scale of $[0 - 1]$, this value is usually taken as 1.

$$PSNR = 10 * \log_{10} \frac{Max_I^2}{MSE} \quad (3.13)$$

Synthetic objects are computer generated surfaces used to simulate real object in the PSP process. Having an ideal digital representation of the object allows to perform a direct comparison between the object and its 3D reconstruction. Here, MSE and PSNR are obtained by directly comparing the matrices that compose both images, the computer-generated object and the 2D representation of the reconstruction obtained by PSP. It is important to mention that the reconstructions used to obtain their metrics were not submitted to a post-processing stage. This, since only the phase unwrapping algorithms are being tested. Table 3.1 show a summary of the average metrics obtained by using synthetic objects. A total of 5 synthetic objects were used to obtain the metrics shown. Notice here, that QG⁷ is not described since it proved poorly efficient when testing synthetic objects. Some of the objects used for this test are shown in figure 3.14.

⁷Quality Guided

Table 3.1: Metrics for the phase unwrapping algorithms using symmetric objects

Synthetic Objects			
Method	MSE	PSNR	Execution Time (seg)
Itoh 2D	31248558509e-08	75.0517001178832	0.138235
Graph Cuts	3.12485585093176e-08	75.0517001178832	72.845235
Constantini	3.12485585107644e-08	75.0517001176822	5.9397588

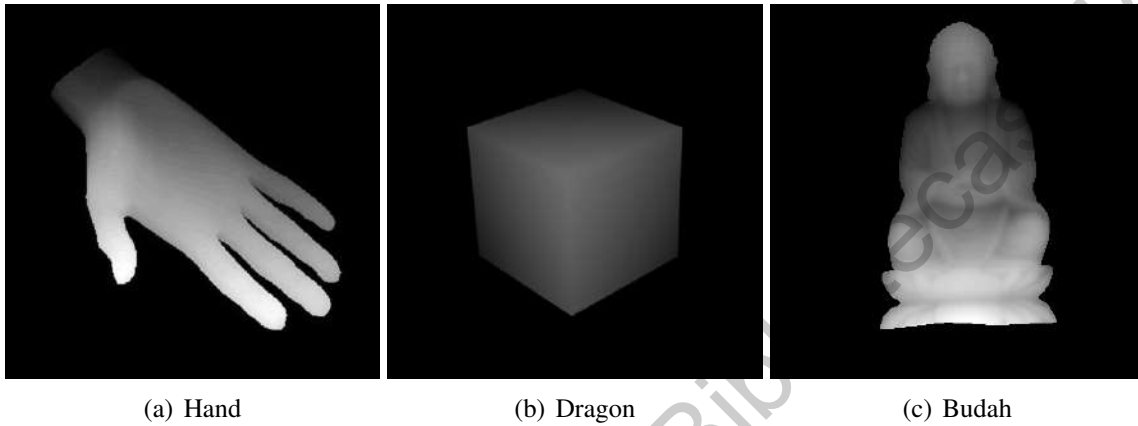
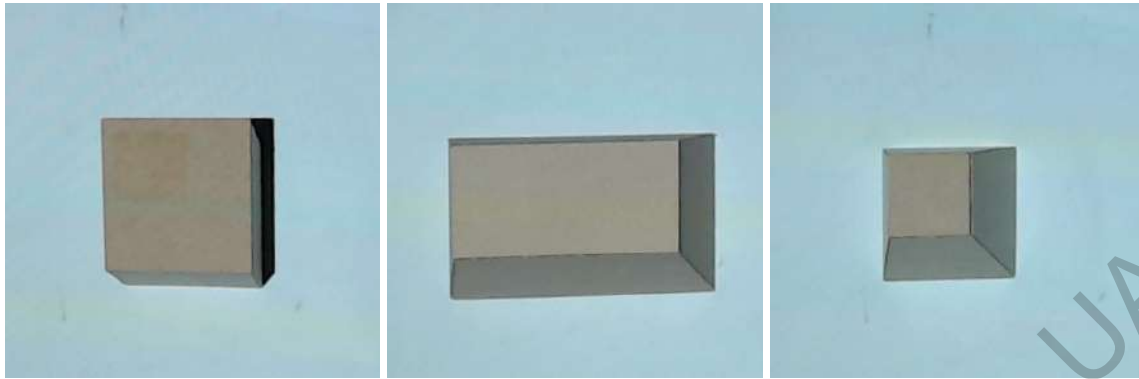


Figure 3.14: Example of synthetic objects used for phase unwrapping analysis

In the case of symmetric objects, a different approach was taken to test the efficiency of the PU algorithms. Since real objects were used in this experiment, a profile analysis was done to obtain the MSE and PSNR. Since all the objects tested have a symmetric and flat surface, an ideal profile was digitally created as a ground truth to test the algorithms. For each object reconstructed, a profile was taken, normalized and compared with the ideal profile to obtain their MSE and PSNR. Table 3.2 shows a summary of the average values obtained in each metric. A total of 6 symmetric objects were tested. Figure 3.15 shows some of the objects used for testing.

Table 3.2: Metrics for the phase unwrapping algorithms using symmetric objects

Symmetric Objects			
Method	MSE	PSNR	Execution Time (seg)
Itoh 2D	0.1808	7.4271	0.422968
Graph Cuts	0.0214	16.6868	61.74066
Constantini	0.0214	16.6914	4.971914
Quality Guided	0.0119	17.1974	104.8208



(a) (b) (c)

Figure 3.15: Example of symmetric objects used for testing

Figure 3.16 shows an analysis by profile of one of the reconstructed objects. Here, it can be seen how each of the algorithms compare to the original shape. Itoh 2D shows the most unfavorable results, while the rest of the algorithms have a better comparative to the original profile, however still showing great levels of noise.

Analysis by profile

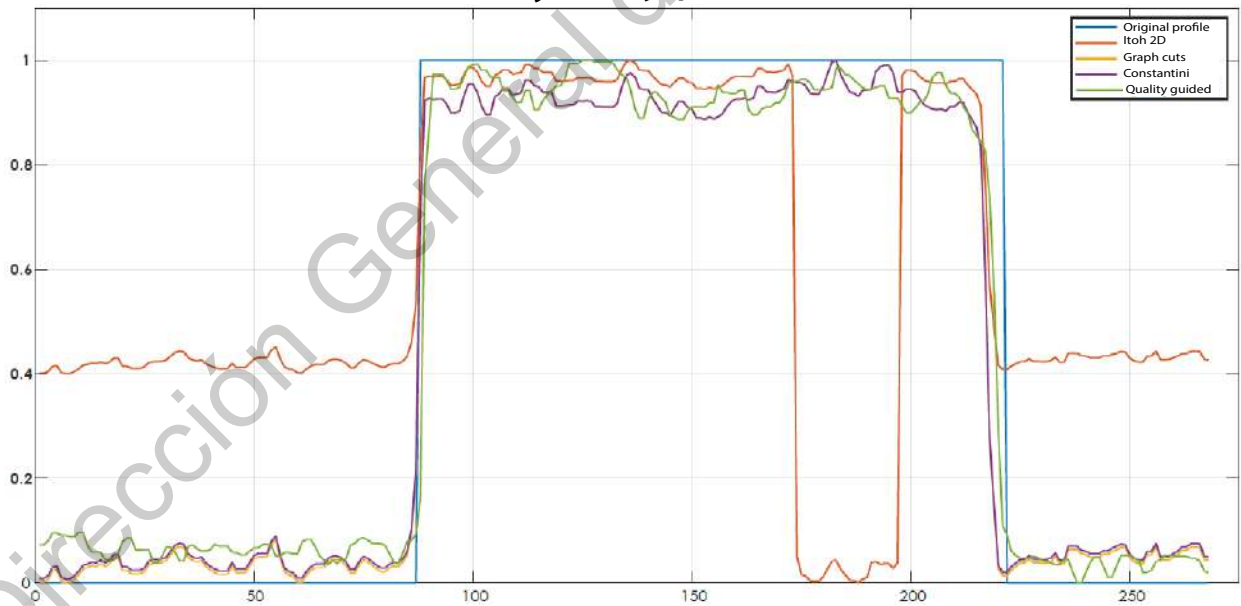


Figure 3.16: Analysis by profile of the performance of PU algorithms in symmetric objects

It is clear from the results obtained, that Itoh 2D is the fastest algorithm, but is not efficient when it comes to doing a satisfactory unwrapping of the phase maps. Although it works perfectly fine in ideal condition, albeit synthetic objects. Quality Guided does a good unwrapping, but at high execution times. Graph cuts and constantini have similar results, but constantini proves to be a much faster method.

3.7 Filtering

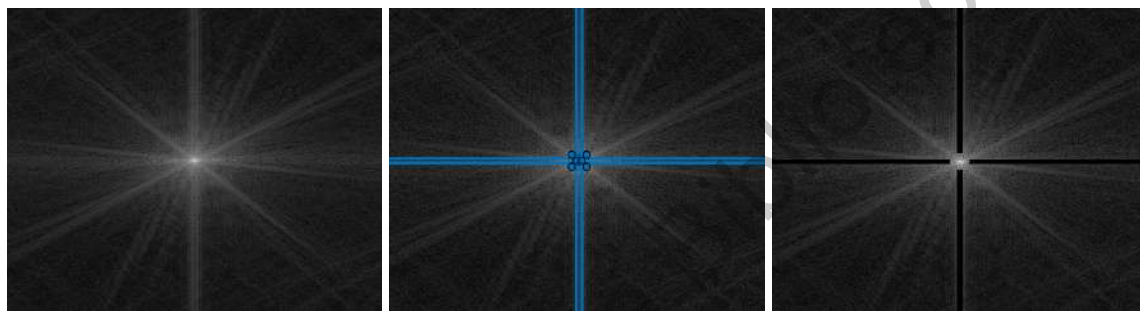
Phase unwrapping is a NP-Hard problem which offers no exact solution to every test case. Therefore, on many occasions the obtained reconstructions may not be satisfactory and contain a consistent persistence of noise. This noise is usually in the form of Moiré patterns.

Since Moiré patterns are formed when two or more periodic rulings are made to overlap, it is only logical that this type of noise may be present during the phase-shifting methods. Since shifted fringe patterns are used to obtain the phase map of the surface, Moiré patterns tend to be carried out during the entire PSP process, from the image acquisition stage and all the way to the phase unwrapping stage. This noise drastically lowers the quality of the reconstructions and it causes height estimations to be inconsistent or to be inaccurate. This is why, it is important to treat Moiré noise at some point during the PSP process. Since, it is very difficult to treat Moiré patterns during the image acquisition stage, or during any other stage of the process for that matter, the present work, proposes the treatment of this noise as a post-processing step. This would allow to work over the final result and improve it by some means.

3.7.1 Cross filter

Over the years, and given the demand for high resolutions 3D reconstructions more and more techniques for the treatment of Moiré noise in images have appeared. Liu(Liu, Yang, & Yue, 2015) proposed a Moiré pattern removal method via low rank and sparse matrix decomposition. However, this technique is used exclusively on texture images with the premise that textures are locally well patterned. Sun(Sun, Yu, & Wang, 2018) also proposed a new approach based on convolutional neural network, achieving state of the art performance to image restoration techniques. In this thesis, an amplitude spectrum analysis is proposed for the treatment of Moiré noise. By filtering the high frequency peaks in the amplitude spectrum of the image, the resulting reconstructions have smoother surfaces and less presence of noise peaks.

A cross filter is used to exclude the noise components from the 3D reconstructions by removing isolated noise or distorted frequencies. Since, vertical fringe patterns are used in fringe analysis, when analyzing the amplitude spectrum the noise components would be normally found along the horizontal axis of the spectrum. However, this may not always be true, since the noise components can be propagated along the entire image spectrum. A cross filter is proposed to exclude not only the components in the x-axis, but also in the y-axis. Figure 3.17 (a) shows an example of an amplitude spectrum where the noise components are found along the horizontal and vertical axis. Figure 3.17 (b) shows the same amplitude spectrum with the corresponding bands for filtering. Finally figure 3.17 (c) shows the resulting spectrum after the filter was applied.



(a) Amplitude spectrum with noise components of both axis (b) Selection of components to be filtered in the spectrum (c) Filtered amplitude spectrum

Figure 3.17: Cross filtering

Since the amplitude spectrum of an image is found in the frequency domain, the filter works with Fourier transform to translate the image to its frequency correspondent. To do this, the filter must receive the 2D representation of the reconstructed surface in grayscale. Thus, the 2D amplitude spectrum can be obtained. Figure 3.18 shows the steps to apply the cross filter to an image.

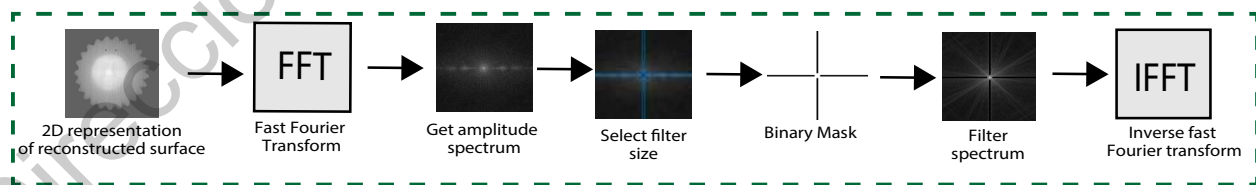


Figure 3.18: Steps to apply cross filter to an image

Algorithm 2 describes the cross filter in greater detail.

Algorithm 2: Cross Filtering

Input: G - Grayscale Image

widthBand - Filter width

Output: C -Grayscale filtered Image

```
1 Set ffta ← FastFourierTransform(G)           // Discrete Fourier Transform
2 Obtain Spectrum
3 Set x ← height(G)
4 Set y ← width(G)
5 Set h ← x - widthBand
6 Set h1 ← Rectangle(0,h,x, widthBand*2)      // Creates horizontal band
7 Set w ← y - widthBand
8 Set h2 ← Rectangle(w,0,widthBand*2,y)      // Creates vertical band
9 Set radius ← 2*(widthBand*2)
10 h3 ← Circle(Center, radius)                // Creates center band
11 Create Mask h1, h2, h3
12 ShiftFourierTransform(ffta) // Shift the zero-frequencies component to the center
13 Set AfftA ← ffta*Mask
14 Set FfftA ← angle(ffta)*Mask
15 fftC ← AfftA*FfftA
16 Set C ← InverseFourierTransform(fftC)      // Inverse Discrete Fourier Transform
17 return C
```

Results

The results are divided in three main sections. The first section shows the results obtained when applying the proposed methodology. The second section focuses on how the two main contributions to the PSP process affect the final 3D reconstruction. The third and final section illustrates a comparison between the proposed methodology in this thesis, the traditional PSP method as well as with other methodologies. All the experiments were tested using Matlab R2019B and Python 3.7.6.

4.1 Database

All images were captured using an in-house capture system. Table 4.1 shows the specifications for the hardware used in the image acquisition stage and the processing of the images.




Device	Brand	Specifications	Image
WebCam	Logitech C920 Pro	<ul style="list-style-type: none"> • HD Webcam • 1080p • 30 frames per second 	
Projector	Asus S1	<ul style="list-style-type: none"> • DLP Projector • 854x480 native resolution • 200 lumens 	
Computer	Dell G3	<ul style="list-style-type: none"> • 16GB RAM • Intel® Core™ i7-8750GHz • Windows 10 64 bits 	

Table 4.1: Devices used for image acquisition

Figure 4.1 shows some of the objects and facial surfaces used for testing. Some of the objects were chosen since they resemble human faces but are static during image acquisition. Symmetrical objects of known dimensions were also used for the analysis of phase unwrapping algorithms and height estimation.

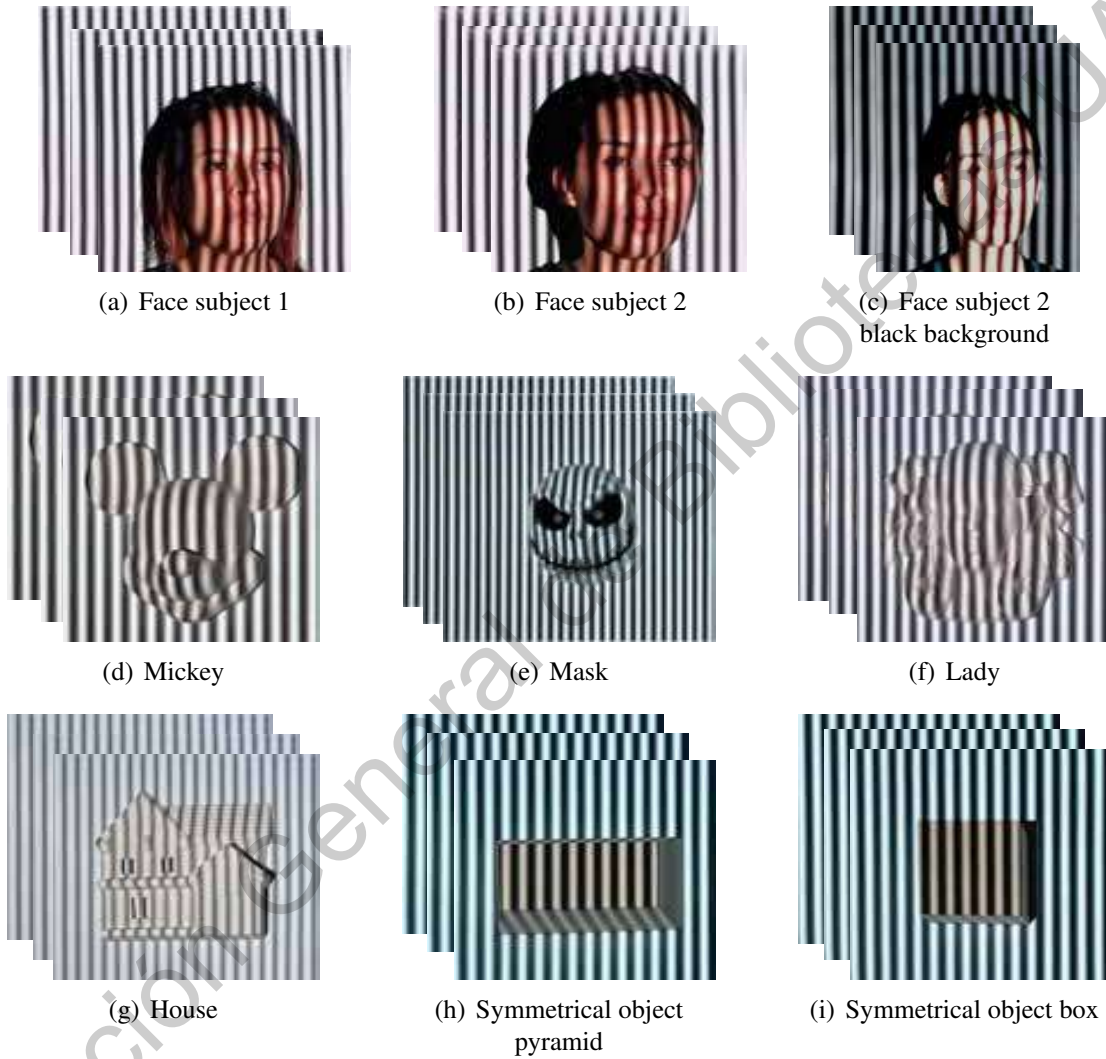


Figure 4.1: Example of some of the surfaces used for testing

4.2 3D reconstructions

Figure 4.2 shows the 3D reconstruction of an object using the proposed methodology. The figure shows the main stages of ROI detection and the creation of the binary mask parting from the original surface. In this particular case a value of $K = 3$ was used since there are three regions detected, the background, the surface and a slight shadow created by the angle of the camera. This object was particularly chosen since it resembles some of the features of a real face, while still being static, which tests particularly well. Images (c) and (d) show a 2D visualization of the reconstruction pre and post cross filtering. Notice how the application of the filter removes some of the Moiré noise found in the surface, specially in the ear of the Mickey.

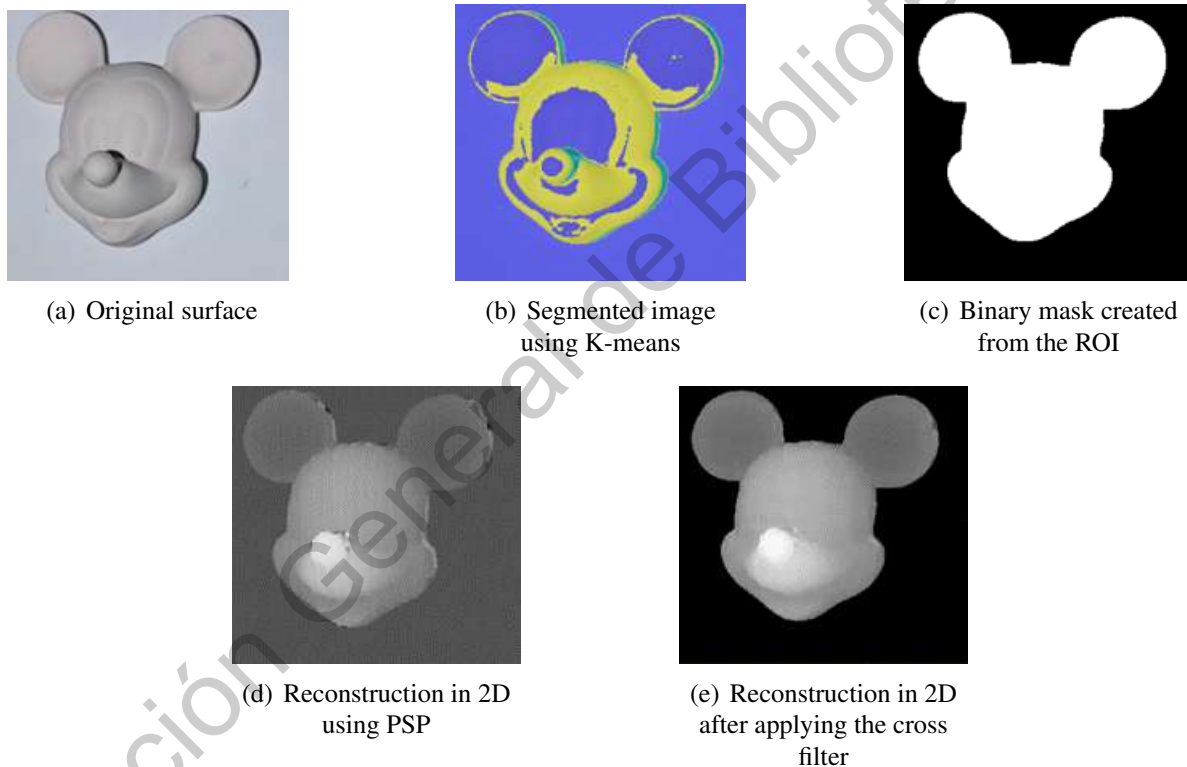


Figure 4.2: 3D reconstruction of an object by stages, visualization in 2D.

Figure 4.3 shows the 3D representation of the reconstruction presented in the previous figure. Here it is more noticeable how the application of the cross filter reduces the high noise peaks, resulting in a much smoother surface. Finally, by adding texture to the final result, it can be seen how well the result approaches the real surface. In this case, the original image, without the fringes, is

superimposed on the reconstructed surface. It is worth mentioning that the data is normalized to a values in the range of [0-1] and a calibration would be needed to obtain the real dimensions of the object at this stage.

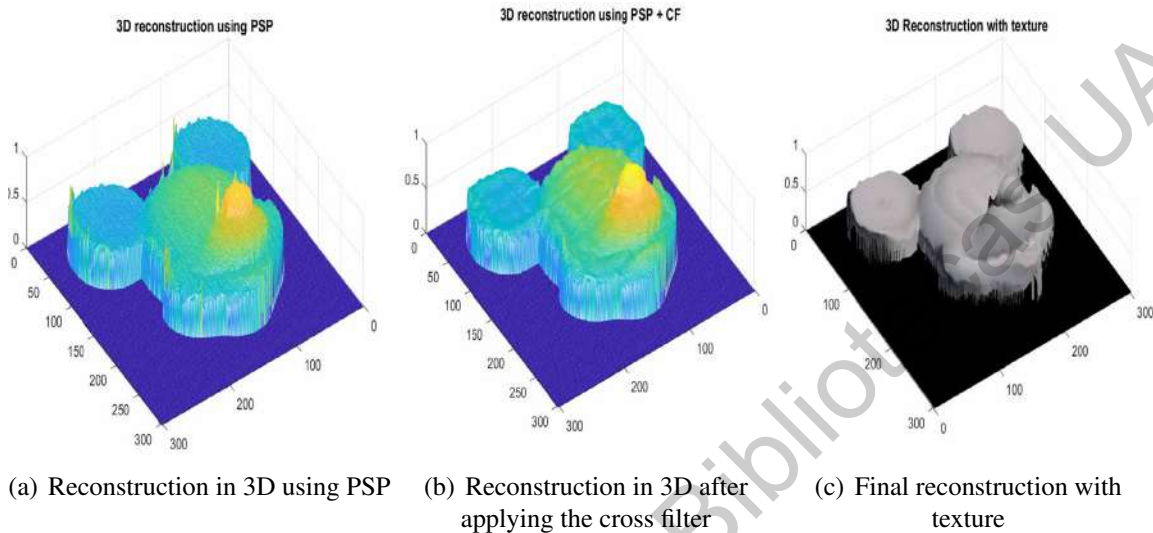


Figure 4.3: 3D reconstruction of an object

One of the more important aspects of the proposed methodology is to test how well it behaves when testing on real faces. In contrast to objects, face capturing can be a bit trickier, since it is important that the subject be as still as possible as to not alter the induced shift in the fringe patterns. Also, ROI detection may be uneven if the subject moves while acquiring the images. Although the process is fairly quick, it was important for the subject to have as little movement as possible during capture.

Figure 4.4 shows a second example of a 3D extraction applied to the human face. In this case, a value of $K = 3$ was also used since there are three main regions detected, the background, the actual face and hair present. This value leads to the binary mask that allows to successfully extract the face contour from the image, since this work is only concerned with the reconstruction of this particular facial area. In image (d) it can be seen how the presence of Moiré noise is more prevalent than in the previous test case, the Mickey mouse. This can be attributed to a slight movement that the subject may have done during image acquisition. However, even though the noise is more present, the characteristics of the facial contour can still be observed. After applying the cross filtering, image (e), most of the noise is reduced, creating a cleaner image. Notice how the

application of the filter does not create any type of loss in the characteristics of the face.

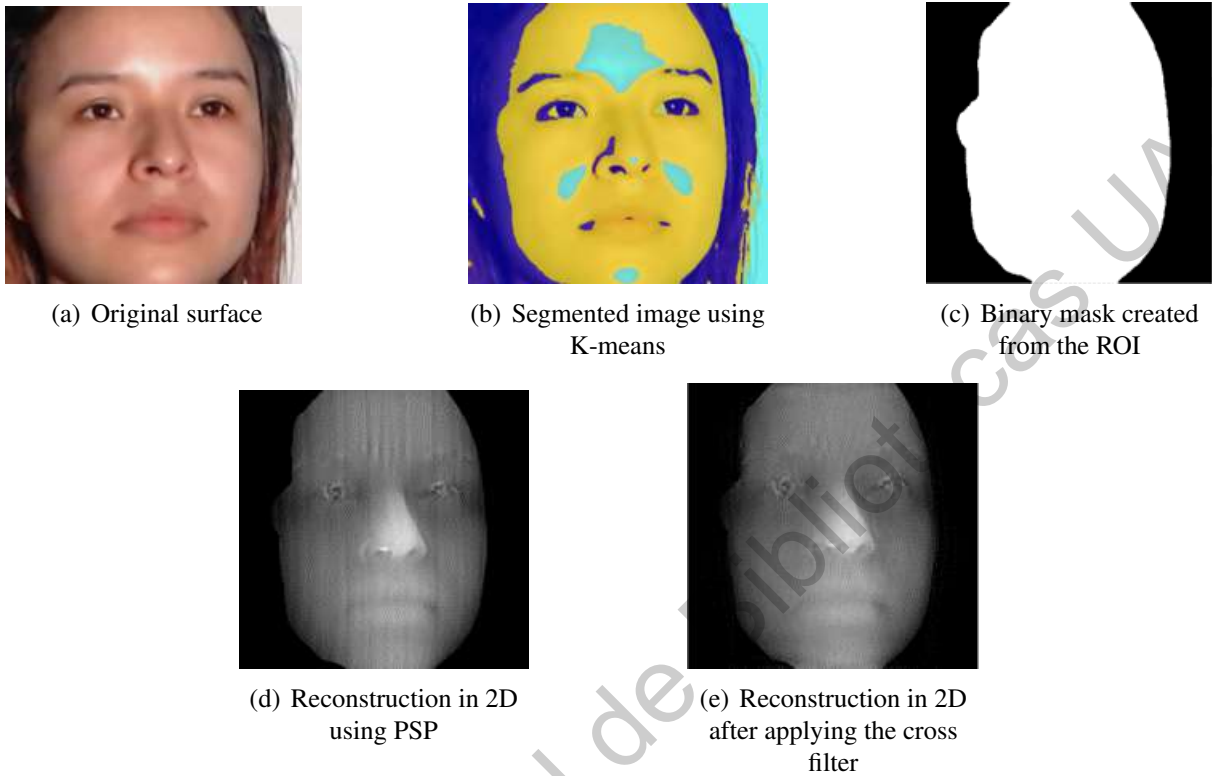


Figure 4.4: 3D reconstruction of a human face, visualization in 2D.

When taking a look at the 3D reconstructions as seen in figure 4.5 it is evident the improvement over the surface that the cross filtering has. Most of the noise in image (a) has been dialed down in image (b), although some can still be seen in some regions, specially the front. Finally in image (c) the final reconstruction can be seen with texture added to it creating the appearance of a real tridimensional facial surface.

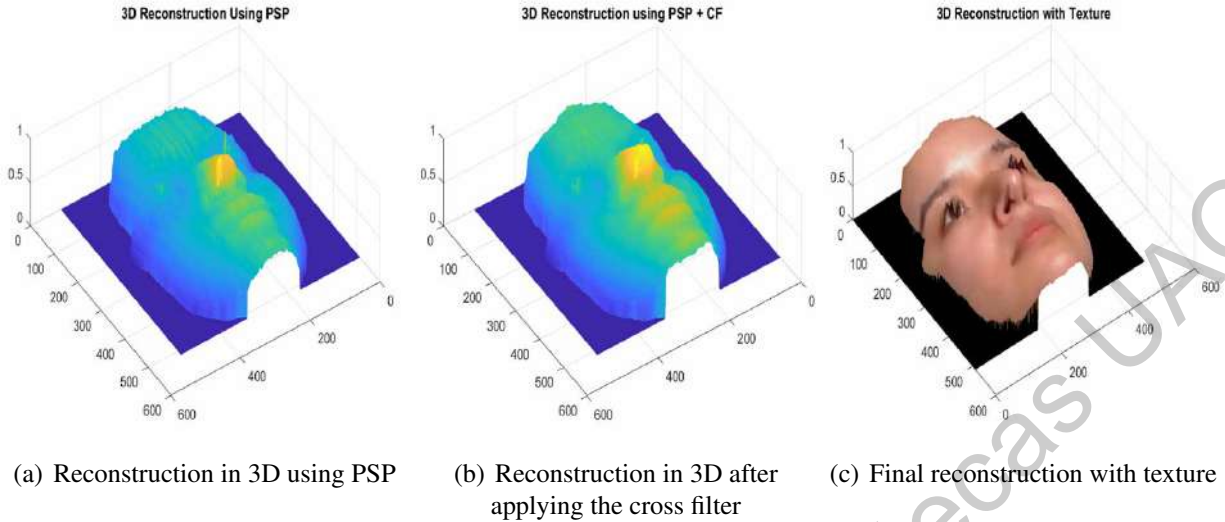


Figure 4.5: 3D reconstruction of an object

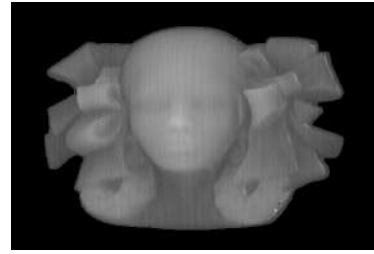
The previous two examples showed that the proposed methodology successfully obtains an accurate tridimensional representation of a surface while maintaining the characteristics of it. It also shows that by applying the cross filter, the resulting surface can be improved without loss of information.

4.3 Impact of ROI detection and cross filtering

ROI detection prevents noise propagation from regions outside the main area of the surface. Cross filter reduces the presence of Moiré noise in the final reconstruction. Both of these stages result in a 3D reconstruction that preserves the details of the original object, while accurately depicting a smooth surface that can be used for 3D measurement. Figure 4.6 shows an example of how both of these contributions alter the final result. The object depicted was specially chosen since it possesses a high level of detail. While some of the details can not be retrieved like the case of the hair splits in the top, these do not alter the final height estimation. Notice how the imaged (d) has a better quality, meaning that both of these stages, ROI detection and cross filtering, greatly impact on the final result.



(a) Original object



(b) PSP + ROI detection



(c) PSP + cross filter



(d) PSP + ROI detection + cross filter

Figure 4.6: Impact of ROI detection and cross filtering in a highly detailed surface

4.3.1 Shadow detection

One of the main contributions of using a region of interest in this work is the detection of shadow. When detecting the ROI those regions that do not contribute to the overall process can be eliminated from the processing images. In PSP shadow is something that is commonly captured when using fringe analysis. Given the concept of triangulation and the use of structured light, it is not a surprise that the shadows are projected onto the background by the surface under study, and then captured by the camera. Since shadows create gaps or holes in the images, shadows means noise. This noise will usually be propagated during the entire PSP process leading to results that are highly inaccurate and that do not represent trustworthy representation of the real object or surface.

Noise created by shadows can be treated before it begins its propagation, by eliminating the shadow regions from the images and only concentrating on the object. When using image segmentation by K-means it is important to consider shadow regions as a cluster. It is important also to choose a background that would highlight the presence of shadows. In this thesis, a white background was usually used to make shadows appear. Once the shadow region is detected it would be easier to extract it from the images using binary morphology.

In figure 4.7 an example of a test where shadows highly affected the overall result is shown. Symmetrical objects were highly prone to create shadows, as can be seen in image (a). Since there is no fringe deformation in the shadow regions, the final reconstruction (b) would appear with gaps that would certainly affect not only the visual quality of the final image, but the height estimations as well. By detecting the shadow region and eliminating it, the propagation of this noise can be stopped. Image (d) shows the final reconstruction when eliminating shadow noise. It is clear that gaps and holes that appeared previously were eliminated, creating a much better result.

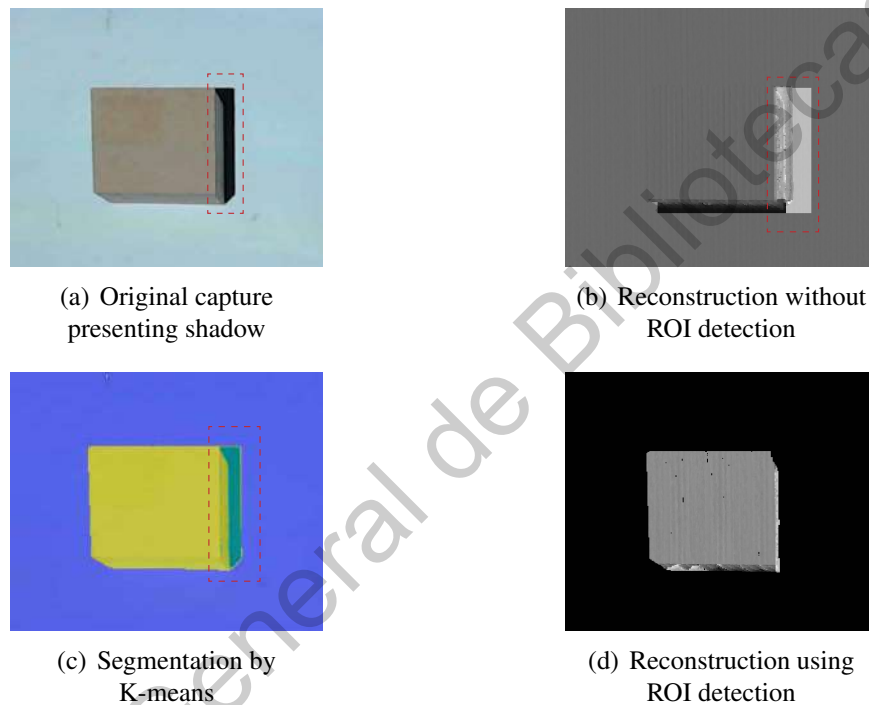


Figure 4.7: Example of shadow exclusion by image segmentation

4.3.2 Cross filtering up close

The proposed cross filter allows to examine the amplitude spectrum of an image to eradicate the unwanted frequencies that cause the quality of the image to be poor. When taking a closer look at figure 4.8, it can be seen that the vertical lines that covered the facial surface in the first image have been soften or even eliminated to a certain level. It is worth noticing how the main features of the facial surface, nose, lips, and eyes have not been tampered with in the resulting image. There is almost no loss of significant information when applying the filter. When visualizing the resulting

surface in three dimensions as in figure 4.5 it is clear that the surface after filtering is smoother, allowing to successfully superimpose texture.

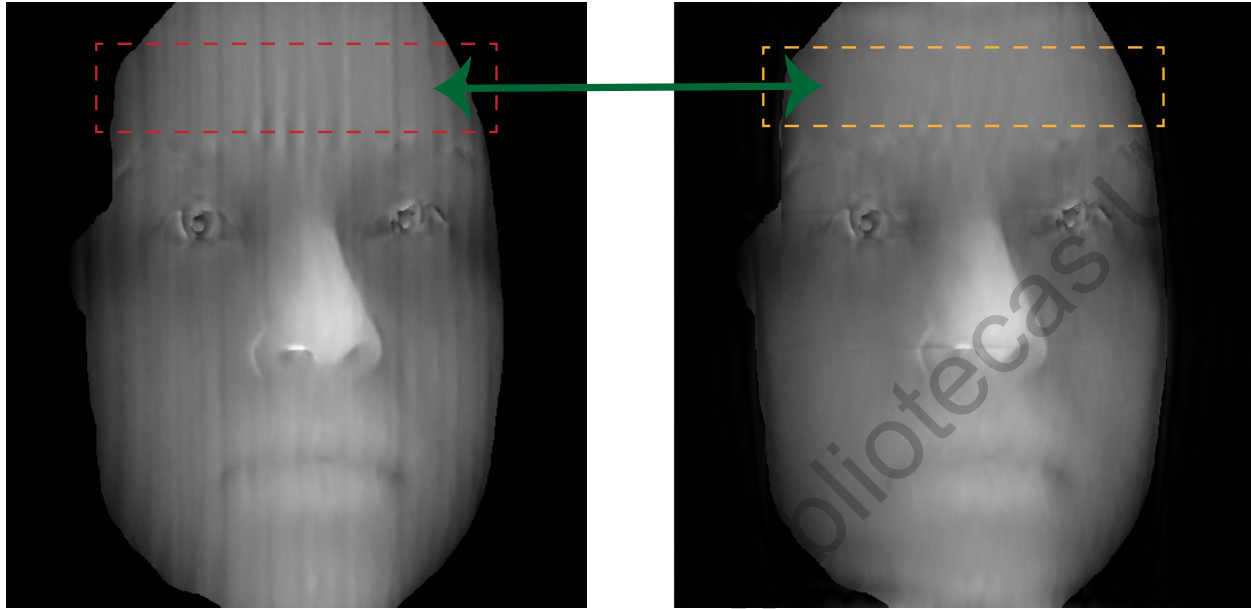


Figure 4.8: A closer look at Moiré noise treatment by cross filter

Figure 4.9 shows a profile analysis of the two previous images. Here, the middle row of the images, both images have the same size, was taken, normalized and plotted. The post-filter profile shows a much smoother, cleaner curve. Moreover, when estimating the real height at certain point in the image, the post-filter profile would throw better estimations. When multiplying the image values by a real size factor and simulating the real dimensions of the surface, having noise peaks would underestimate the real height in certain regions of the image. By eliminating these peaks, the highest point in the 3D surface would correctly estimate the actual size of the real object or surface.

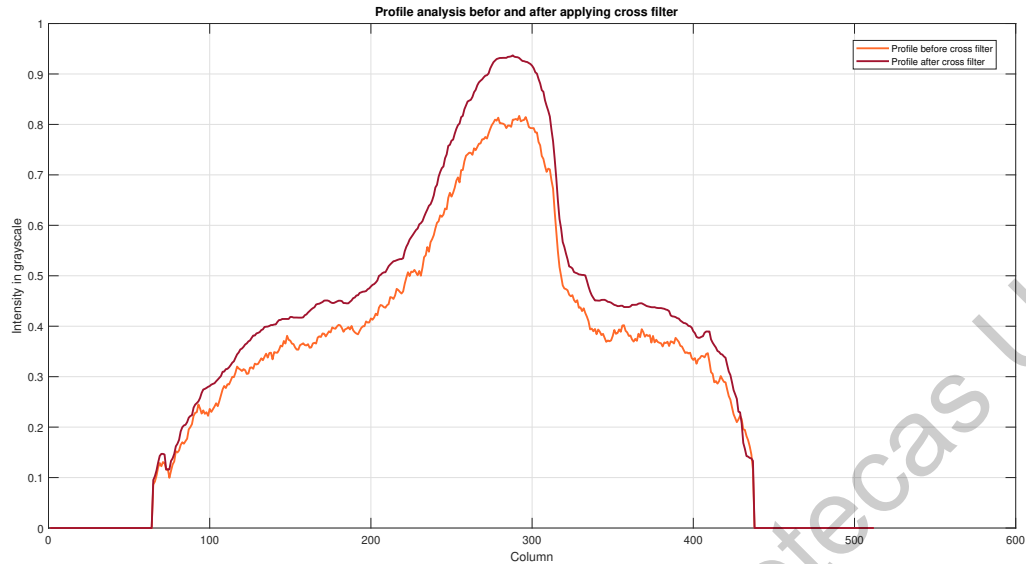


Figure 4.9: Profile analysis of a 3D reconstruction before and after applying cross filter

4.4 Comparative with other methods

The proposed methodology in this work, is based on the traditional PSP method for 3D extraction. When comparing the proposed method with the traditional approach, it was discovered that the proposed method would obtain better results in terms of visual quality of the 3D reconstructions and when estimating the real height of the objects. In this section, the proposed method is compared with the traditional PSP model, but also with the model proposed by Escobar (Escobar, 2016) in 2016. In his work, Escobar uses the traditional PSP but contributes to it, by adding an algorithm to eliminate discontinuities after the phase unwrapping algorithm. To successfully obtain a fair comparison between these three models, two tests were created. The first test consists of obtaining a 3D reconstruction of a human face to compare the visual quality of the three results. The resulting images visualized in 2D can be seen in figure 4.10.

It can be seen here, that the appropriate extraction of the region of interest affects greatly to the overall result. While the reconstruction done by the method proposed by Escobar somewhat improves on the traditional method, it still does not offer a satisfactory high resolution reconstruction. Most of the information obtained by the first two models can be considered noise, Moiré noise is specially present. Also, the hair of the person may play an important factor in obtaining unsatisfactory results. Since there is almost no deformation by this feature in the fringes, the phase

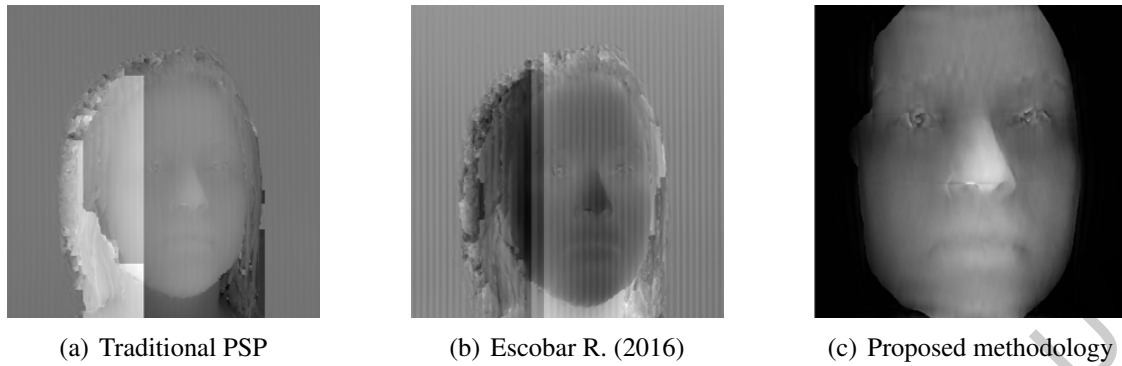


Figure 4.10: Comparative of a reconstructed surface by various methods visualized in 2D.

extraction and unwrapping is specially complicated. Thus, leading to the propagation of noise to the actual facial contour. Furthermore, the presence of shadows creates holes in certain zones of the image that drastically lower their quality. Figure 4.11 shows these same reconstructions in a tridimensional perspective.

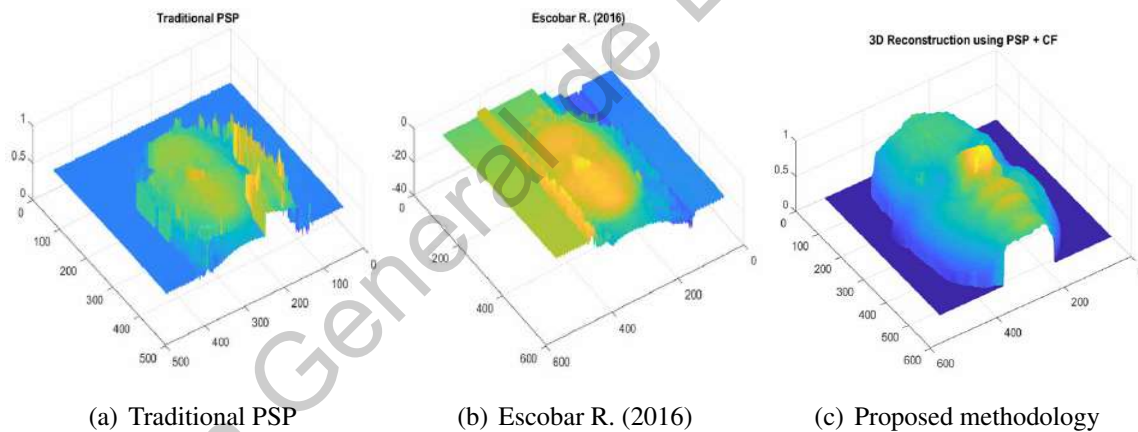


Figure 4.11: Comparative of a reconstructed surface by various methods visualized in 3D.

The second test was performed using symmetric objects. Since the real dimensions of these objects are known, a 3D representation of this can be generated virtually. In this case, a profile analysis was performed to test the accuracy of the proposed methodology with the other two models in terms of height measurement. For this, an ideal profile, normalized in the range of $[0, 1]$ was created for each of these objects. Once the object was reconstructed by all three of these methods, a profile was taken from the final result and directly compared with the virtual profile. All values were normalized to the same range in order to obtain average metric values. A total of 6 objects

were used, where the height of each object is taken a 1.

As it can be seen from table 4.2, the proposed method has a lower error when obtaining an average height. While the traditional method has a high error of 22%, the proposed method lowers this error by 11%. Furthermore, the metrics shown also incline in favor of the proposed method against the method proposed by Escobar.

Metric	Traditional Method	Escobar (2016)	Proposed Method
Average Height	0.7808	0.8236	0.8914
Difference in Height	0.2198	0.1764	0.1086
Error percentage	21.98%	17.67%	10.86%
MSE (Profile)	0.0485	0.0124	0.0116
PSNR (Profile)	13.1404	15.0403	17.8014

Table 4.2: Height metrics comparative with other methods

Conclusions and future work

5.1 Conclusions

3D extraction is one of the main areas of research in computer science. It deals with the detection of depth in 2D images to model the real life dimensions of surfaces in a digital representation. There are a number of methods that allow to extract the depth information from scenes. These methods can be divided in contact and no-contact techniques. The present thesis presents a methodology based on phase-shifting profilometry or PSP, specifically the three-step method, which is a non-contact technique, to reconstruct facial and non-facial surfaces. PSP is a structured-light based technique which uses fringe analysis to project three or more sinusoidal fringe patterns onto a surface. The 3D information of the surface can be retrieved using phase extraction and phase unwrapping generating a 3D reconstruction.

The present work describes in detail each of the stages necessary to successfully reconstruct a surface using PSP. From the image acquisition stage, the pre-processing of the images, the phase extraction and the phase unwrapping and post-processing. It also presents some of the more common phase unwrapping algorithms and illustrates an analysis that evaluates them in terms of speed and performance in the scope of PSP. For this analysis, computer generated and real object were used and the algorithms were evaluated using two metrics: MSE and PSNR.

This thesis takes the traditional PSP method and complements it by adding two main contributions which improve on the reconstructions obtained. The first contribution consists of detecting the region of interest, ROI, by using image segmentation by K-means and binary morphology. By limiting the image to only the ROI, error propagation acquired during image acquisition is reduced

in the phase unwrapping stage. This step is used as a preprocessing stage and applied before phase extraction and phase unwrapping.

The second contribution consists of a cross filter used as a post-processing stage that filters Moiré noise that results from using multiple fringe shifted in phase fringe patterns. This filter, uses the 2D representation of the reconstructed surface and filters its amplitude spectrum in the frequency domain. The Moiré noise is filtered by applying a binary mask in the shape of a cross to eliminate the noise peaks that can be found in the horizontal axis, as well as the vertical axis. The use of this filter proved to improve the reconstructed surfaces by attenuating the presence of noise resulting in improvement of quality.

The results obtained showed that the proposed methodology achieves better results than the traditional PSP method. By limiting the region in the images and by applying a filter to attenuate Moiré noise, the resulting 3D reconstructions present better image quality. Moreover, a profile analysis of symmetrical objects of known dimensions proved that the proposed method achieves better measurement estimation than the traditional PSP by 11%. The method was tested using real objects and surfaces, specially human faces to simulate a real life application.

In conclusion, this work present the development and implementation of a methodology to successfully reconstruct real-life surfaces in three dimensions parting from 2D images. The proposed methodology is based on the PSP method but improves on it by adding two additional steps with the purpose of obtaining high quality 3D reconstructions.

5.2 Recommendations for Future Work

The work allows for future contributions which could improve even more in the results. The main contributions may be during the image acquisition stage by creating an automatic capture system. Another contribution may be done in the post-processing stage by testing other existing or new filters that would allows to attenuate or reduce Moiré noise, not only by amplitude spectrum analysis.

Other important areas of improvement that can lead to interesting research can be found below. The use of AI techniques is specially encouraged since they have proven to be extremely successful in computer vision.

- Combine the proposed methodology with phase unwrapping methods based in support vector

machines or SVM.

- Phase extraction by deep learning.
- Surface smoothing filters as part of the post-processing stage of the process.
- Compare with other 3D extraction techniques.
- Test the reconstructed facial surfaces in a face authentication system.

Dirección General de Bibliotecas UAQ

References

- Alvarado Escoto, L. A., Ortega, J. C. P., Ramos Arreguin, J. M., Gorrostieta Hurtado, E., & Tovar Arriaga, S. (2020). The effect of bilateral filtering in 3d reconstruction using psp. In M. F. Mata-Rivera, R. Zagal-Flores, & C. Barria-Huidobro (Eds.), *Telematics and computing* (pp. 268–280). Cham: Springer International Publishing.
- Bioucas-Dias, J., & G., V. (2007). Phase unwrapping via max flows. *Image Processing, IEEE transactions*, 698-709.
- Dai, J., Li, B., & Zhang, S. (2014). High quality three-dimensional (3d) shape measurement using intensity-optimized dithering technique. *Optics and Lasers in Engineering*, 53, 79-85. doi: 10.1016/j.optlaseng.2013.08.015
- Escobar, R. (2016). *Digitalización de sólidos utilizando análisis de franjas y técnicas de desplazamiento de fase en arquitecturas arm* (Unpublished master's thesis).
- Fernandez, S., & Salvi, J. (2013). Handbook of 3d machine vision. optical metrology and imaging. In S. Zhang (Ed.), (1st ed., p. 101-150). Boca raton: CRC Press.
- Gdesait, M., & Lilley, F. (2012). Two-dimensional phase unwrapping problem.
- Gong, Y., & Zhang, S. (2010). Ultrafast 3-d shape measurement with an off-the-shelf dlp projector. *Opt. Express*, 18(19), 19743–19754. doi: 10.1364/OE.18.019743
- Gonzalez, A. (n.d.). *Morfología de imágenes binarias*.
- Gorthi, S. S., & Rastogi, P. (2010, 02). Fringe projection techniques: Whither we are? *Optics and Lasers in Engineering*, 48. doi: 10.1016/j.optlaseng.2009.09.001
- Guo, H., He, H., & Chen, M. (2004, 06). Gamma correction for digital fringe projection profilometry. *Applied Optics*, 43, 2906-14. doi: 10.1364/AO.43.002906
- Haralick, R. M., & Shapiro, L. G. (1985). Image segmentation techniques. *Computer Vision, Graphics, and Image Processing*, 29(1), 100 - 132.
- Huang, P., Hu, Q. J., & Chiang, F. (2002). Double three-step phase-shifting algorithm. *Applied optics*, 41, 4503-4509.

- Jun-ichi, K. (2015). Handbook of optical metrology. principles and applications. In Y. Toru (Ed.), (2nd ed., p. 49-510). CRC Press.
- Lehmann, E., & Casella, G. (1998). *Theory of Point Estimation*. Springer Verlag.
- Li, Y., & Wu, H. (2012). A clustering method based on k-means algorithm. *International conference on solid state devices and material science*.
- Lin, H., Si, J., & Abousleman, G. P. (2007). Region-of-interest detection and its application to image segmentation and compression. In *2007 international conference on integration of knowledge intensive multi-agent systems* (p. 306-311). doi: 10.1109/KIMAS.2007.369827
- Liu, F., Yang, J., & Yue, H. (2015). Moiré pattern removal from texture images via low-rank and sparse matrix decomposition. In *2015 visual communications and image processing (vcip)* (p. 1-4). doi: 10.1109/VCIP.2015.7457907
- Mohammadi, F., Madanipour, K., & Rezaie, A. H. (2012). Accuracy enhancement of 3d profilometric human face reconstruction using undecimated wavelet analysis. *Appl. Opt.*, *51*(16), 3120–3131. doi: 10.1364/AO.51.003120
- Nguyen, H., Kieu, H., Wang, Z., & Le, H. (2018). Three-dimensional facial digitization using advanced digital image correlation. *Applied Optics*, *57*, 2188. doi: 10.1364/AO.57.002188
- Oster, G., & Nishijima, Y. (1963). Moiré patterns. *Scientific American*, *208*(5), 54–63.
- Ou, P., Li, B., Wang, Y., & Zhang, S. (2013). Flexible real-time natural 2d color and 3d shape measurement. *Opt. Express*, *21*(14), 16736–16741. doi: 10.1364/OE.21.016736
- Prof, L., Saupe, D., & Hamzaoui, R. (2001, 05). Fractal image compression.
- Raj, S., Raj, S., & Kumar, S. (2015, 07). An improved histogram equalization technique for image contrast enhancement..
- Salvi, J., Fernandez, S., Pribanic, T., & Llado, X. (2010). A state of the art in structured light patterns for surface profilometry. *Pattern Recognition*, *43*, 2666-2680. doi: 10.1016/j.patcog.2010.03.004
- Sansoni, G., Corini, S., Lazzari, S., Rodella, R., & Docchio, F. (1997, Jul). Three-dimensional imaging based on gray-code light projection: characterization of the measuring algorithm and development of a measuring system for industrial applications. *Appl. Opt.*, *36*(19), 4463–4472. doi: 10.1364/AO.36.004463
- Schreiber, H., & Bruning, J. (2006). Optical shop testing. In D. Malacara (Ed.), (3rd ed., p. 547-666). Wiley interscience. doi: 10.1002/9780470135976.CH14
- Sun, Y., Yu, Y., & Wang, W. (2018, Aug). Moiré photo restoration using multiresolution convolutional neural networks. *IEEE Transactions on Image Processing*, *27*(8), 4160–4172. Retrieved from <http://dx.doi.org/10.1109/TIP.2018.2834737> doi: 10.1109/tip.2018

.2834737

- Syakrani, N., Mengko, T., Suksmono, A., & E.T., B. (2007). Comparison of puma and cunwrap to 2-d phase unwrapping. *Proceeding of the 2011 international conference of electrical engineering and informatics.*, 1-6.
- Szeliski, R. (2010). *Computer vision: Algorithms and applications* (1st ed.). Berlin, Heidelberg: Springer-Verlag.
- Takeda, M., & Mutoh, K. (1983). Fourier transform profilometry for the automatic measurement of 3-d object shapes. *Appl. Opt.*, 22(24), 3977–3982. doi: 10.1364/AO.22.003977
- Van der Jeught, S., & Dirckx, J. (2016). Real-time structured light profilometry: A review. *Optics and Lasers in Engineering*, 87. doi: 10.1016/j.optlaseng.2016.01.011
- Vila, K., Arranz, A., & Alvar, M. S. (2009). *Reconstrucción 3d de modelos utilizando técnicas de visión artificial proyecto de fin de carrera* (Unpublished master's thesis).
- Wei, Z., Wang, J., Nichol, H., Wiebe, S., & Chapman, D. (2011, 07). A median-gaussian filtering framework for moire pattern noise removal from x-ray microscopy image. *Micron (Oxford, England : 1993)*, 43, 170-6. doi: 10.1016/j.micron.2011.07.009
- Xianyu, S., & Chen, W. (2001). Fourier transform profilometry; a review. *Optics and Lasers in Engineering*, 35, 263-284.
- Yagnik, J., Siva, G. S., Ramakrishnan, K., & Rao, L. R. (2005). 3d shape extraction of human face in presence of facial hair: A profilometric approach. In *Tencon 2005 - 2005 ieee region 10 conference* (p. 1-5). doi: 10.1109/TENCON.2005.301088
- Zaid, A. (2008). *Fringe pattern analysis using wavelet transforms* (Unpublished master's thesis).
- Zhao, W.-L., Deng, C.-H., & Ngo, C.-W. (2018). k-means: A revisit. *Neurocomputing*, 291, 195 - 206.